Improving immunotherapy for melanoma: models, biomarkers and regulatory T cells

Rao, D.

Chapter 6

Acidity-mediated induction of FoxP3^{+} regulatory T cells

Disha Rao[1], Johanna A. Stunnenberg[1], Ruben Lacroix[1], Petros Dimitriadis[1], Joanna Kaplon[2], Fabienne Verburg[1], Paula T. van Royen[1], Esmée P. Hoefsmit[1], Kathrin Renner[3,4], Christian U. Blank[1,5,6], Daniel S. Peeper[1,7]

Abstract

Glucose limitation and increased lactic acid levels are consequences of the elevated glycolytic activity of tumor cells, and constitute a metabolic barrier for the function of tumor infiltrating effector immune cells. The immune-suppressive functions of regulatory T cells (Tregs) are unobstructed in lactic-acid rich environments. However, the impact of lactic acid on the induction of Tregs remains unknown. We observed increased TGFβ-mediated induction of Forkhead box $P3^+$ ($FoxP3^+$) cells in the presence of extracellular lactic acid, in a glycolysis-independent, acidity-dependent manner. These $CD4^+$ $FoxP3^+$ cells expressed Treg-associated markers, including increased expression of CD39, and were capable of exerting suppressive functions. Corroborating these results *in vivo*, we observed that neutralizing the tumor pH by systemic administration of sodium bicarbonate (NaBi) decreased Treg abundance. We conclude that acidity augments Treg induction and propose that therapeutic targeting of acidity in the tumor microenvironment (TME) might reduce Treg-mediated immune suppression within tumors.

Introduction

Tumor cells have increased aerobic glycolysis, whereby glucose is converted to lactate despite the presence of oxygen, also termed the "Warburg effect" [1]. Lactate is exported from the cells via proton-coupled monocarboxylate transporters (MCT), which co-transport lactate and protons (thus forming lactic acid) [2]. Consequently, the tumor microenvironment (TME) is characterized by low glucose and high lactic acid levels [3]. High levels of extracellular lactic acid lowers pH values in patient tumors to 6.9-7.0, compared with the physiological pH of 7.3-7.4 in peripheral tissues [4]. In mice, which have a blood pH in the range of 7.1-7.2, the tumor pH is known to be as low as 6.2 [5–7]. Furthermore, pro-inflammatory immune cells are also known to engage aerobic glycolysis [8]. Therefore, an acidic pH, due to high extracellular lactic acid levels, occurs not only in the tumor but also at sites of chronic inflammation [8–11]. Such low glucose and high lactic acid environments often pose a metabolic challenge to infiltrating effector T cells, impairing their proliferation and cytokine production [3, 7, 12–15]. These inhibitory effects are attributed mainly to the impairment of glycolysis in effector T cells, due to intracellular build-up of lactate [13].

In contrast, the survival and immune-suppressive function of regulatory T cells (Tregs) are known to be unhindered in lactic acid-rich environments, owing to their altered metabolism compared with effector T cells [16–18]. Tregs are characterized by the expression of transcription factor Forkhead box P3 (FoxP3), and play an important role in maintaining peripheral tolerance [19]. However, due to the suppression of effector T cells and dendritic cells, the presence of Tregs in the tumor is associated with poor prognosis in several cancer types [20, 21]. The expression of FoxP3 is known to cause a shift in metabolism of Tregs towards reduced glycolysis and increased oxidative phosphorylation (OXPHOS) [22, 23]. Indeed, Tregs rely on OXPHOS to generate energy and for suppressive functions [24]. On the other hand, the proliferation and migration of Tregs requires glycolysis [23, 25].

FoxP3+ Tregs can be either thymus-derived (tTregs) or peripherally induced (iTregs), and both subsets are involved in suppressing anti-tumor immune responses [26, 27]. Conversion of conventional CD4+ T cells (Tconv) to iTregs (also known as iTreg induction) involves T cell receptor stimulation [28], which in turn necessitates quiescence exit of Tconv cells [29]. This process of quiescence exit is tightly regulated by metabolic cues from the environment, such as increased glucose uptake and glycolysis [29]. It has been suggested that glycolysis is also required for the induction of Tregs from Tconv cells in the periphery [30, 31]. Thus, the presence of lactic acid during stimulation could influence conversion to FoxP3+ Tregs.

As outlined above, Tregs are known to be dependent on glycolysis for induction, migration and proliferation, while OXPHOS is essential for their survival, and immune-

suppression [23–25]. The impact of lactic acid on each process might be different and should therefore be independently evaluated. Although it has been shown that pH-neutral sodium lactate causes an increased Treg induction [22], the additional effect of acidity must also be considered, since it is an important characteristic of lactic acid-rich environments [9, 32]. We therefore evaluated the effect of lactic acid on induction of Tregs. Understanding this will shed light on potential advantages for Tregs in high lactic acid conditions such as the TME, which in turn might provide additional avenues for research aiming to therapeutically target Tregs.

Results

Increased induction of FoxP3$^+$ cells in the presence of lactic acid

We first determined whether the presence of extracellular lactic acid alters the induction of Tregs *in vitro,* using CD4$^+$ CD25$^-$ Tconv cells sorted from spleen of C57BL/6 mice. Addition of TGFβ during stimulation of Tconv cells is known to result in Treg induction [33]. To this setting, we added lactic acid at a concentration of 10 mM, which lowered the pH of media to 6.8, and these levels have been reported to occur in patient tumors [3, 4]. Addition of lactic acid resulted in a 1.4-fold increase in the frequency **(Fig 1A-B, S1A)** and an increase in absolute counts **(Fig 1C)** of FoxP3$^+$ cells. TGFβ was essential for the lactic acid-mediated increase in FoxP3$^+$ cells, since there was no FoxP3$^+$ induction across any groups in the absence of TGFβ during stimulation **(Fig 1A, S1B)**.

We then investigated if the observed increase in frequency of FoxP3$^+$ cells was due to a better survival, or rather resulted from a proliferative advantage in the presence of lactic acid. However, live cell percentages deduced using dead cell stain in the pregated subsets **(Fig S1C)** revealed that there was no difference in viability of FoxP3$^+$ cells in the presence of lactic acid **(Fig 1D)**. Notably, the viability of the FoxP3$^+$ population was higher compared with that of the FoxP3$^-$ populations, but this effect was not mediated by the presence of lactic acid **(Fig 1D)**. Moreover, there was no reduction in viability of FoxP3$^-$ T cells in the presence of lactic acid, irrespective of TGFβ addition **(Fig 1D, S1C)**. We then measured the proliferation of FoxP3$^+$ and FoxP3$^-$ subsets **(Fig S1A)** based on dilution of CellTrace™ Violet (CTV). Lactic acid did not impact the proliferation of either cell type **(Fig 1E, S1D)**. Thus, a proliferative advantage cannot explain the impact of lactic acid on the frequency of FoxP3$^+$ cells. We therefore concluded that the presence of extracellular lactic acid results in an increased conversion of Tconv cells to FoxP3$^+$ cells.

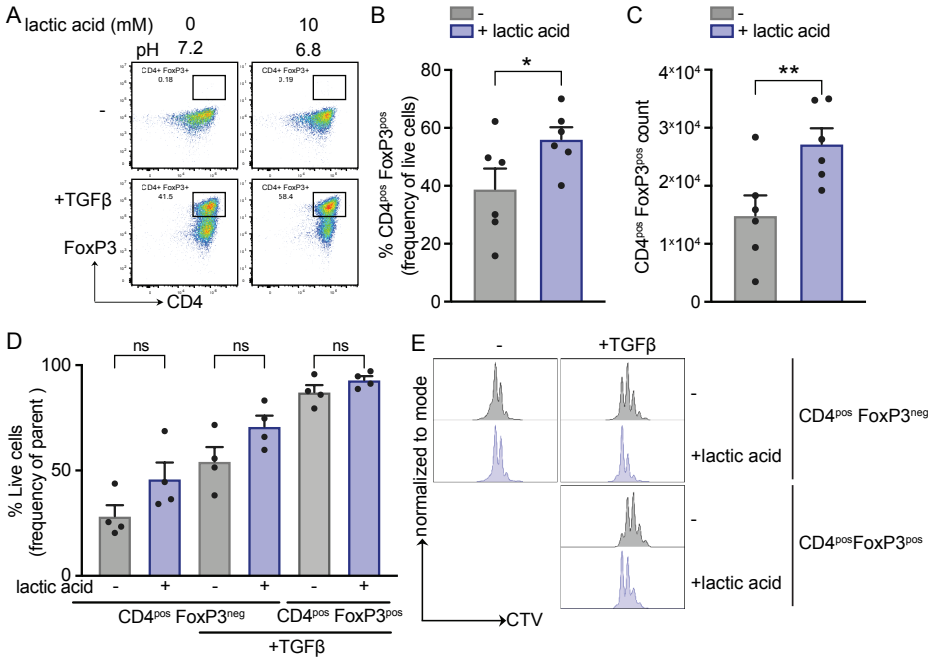

Fig 1: Increased induction of FoxP3⁺ cells in the presence of lactic acid
(A-E) Sorted CD4⁺CD25⁻ Tconv cells obtained from spleens of C57BL/6 mice were stimulated in the presence of 10 mM lactic acid with/without TGFβ (3 ng/ml) for 72h. (A) Representative flow cytometry plots indicating expression of CD4 and FoxP3 across conditions after 72h stimulation. Cells were pre-gated based on scatter and then doublets were excluded, followed by exclusion of dead cells (gating strategy in S1A). (B) Percentage of FoxP3⁺ cells and (C) absolute counts of FoxP3⁺ cells measured using Intellicyt, after 72h stimulation in the presence of TGFβ. (n=6 independent experiments with each experiment containing technical replicates). (D) Live cell frequency within each population was estimated by gating first for expression of CD4 and FoxP3 as indicated, and then excluding dead cells. Percentage of live cells as frequency of respective parent population (gating strategy in S1C; n=4 independent experiments with each experiment containing technical replicates). (E) Representative CellTrace™ Violet dilution plots after gating live cell populations for expression of CD4 and FoxP3 as indicated (representative data of n=3 independent experiments with each experiment containing technical replicates). Each dot is one independent experiment. pos (+); neg (-); Error bars represent SEM. Statistical significance was determined using two-tailed paired Student's t-test (for B-C) or using one-way ANOVA followed by Sidak's multiple comparisons test (for D). ns not significant, * *p*-value<0.05, ** *p*-value<0.01.

Lactic acid-mediated increase in FoxP3⁺ cells is independent of their glycolytic profile

The presence of lactic acid is known to disrupt glycolysis in CD4⁺ and CD8⁺ T cells [13, 34]. We therefore assessed whether lactic acid-mediated conversion of Tconv cells to FoxP3⁺ cells involves a shift in metabolism towards reduced glycolysis. For this, the glycolysis inhibitor 2-deoxy-D-glucose (2-DG) was added during stimulation. We first tested if the dose of 2-DG (0.5 mM) was sufficient to reduce glycolysis in CD4⁺ T cells. Upon stimulation of CD4⁺ T cells without TGFβ, in the presence of 2-DG, we observed reduced glucose uptake **(Fig S2A-B)** and a concomitant reduction in extracellular acidification by CD4⁺ T

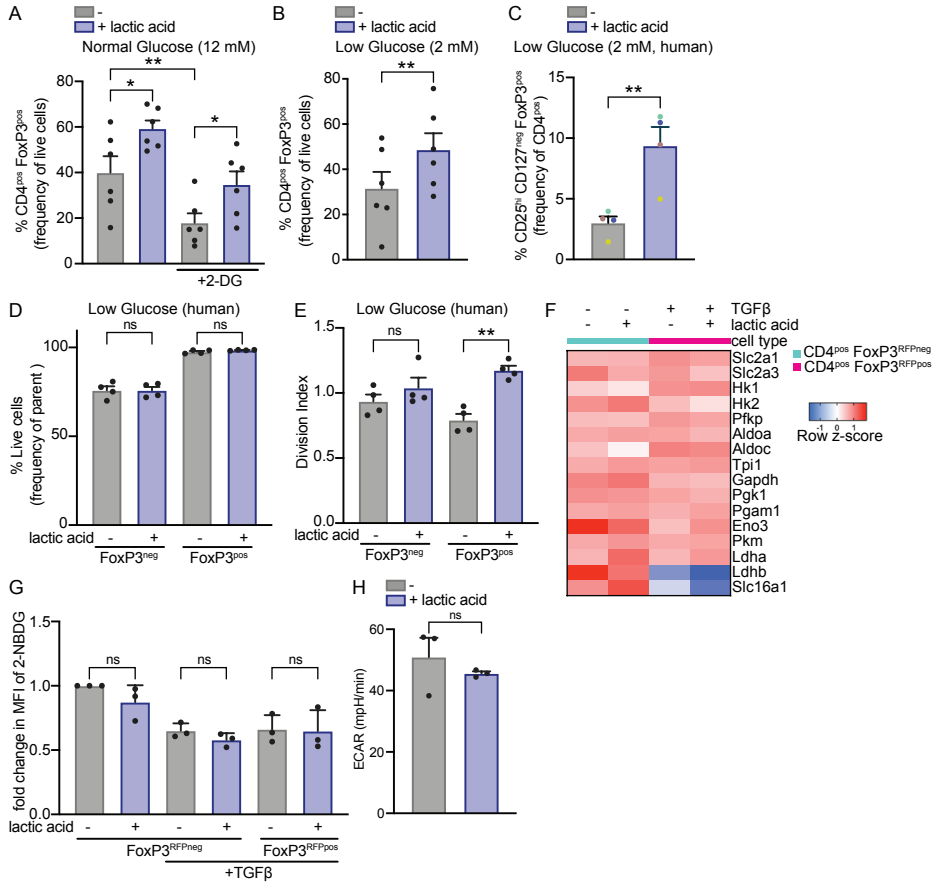

Fig 2: Lactic acid-mediated increase in FoxP3⁺ cells is independent of their glycolytic profile
(A) Percentage of FoxP3⁺ cells induced using sorted CD4⁺CD25⁻ Tconv cells obtained from spleens of C57BL/6 mice in the presence of lactic acid (10 mM) and 2-DG (0.5 mM) for 72h (n=6 independent experiments with each experiment containing technical replicates). (B) Percentage of FoxP3⁺ cells induced using sorted CD4⁺ CD25⁻ Tconv cells obtained from spleens of C57BL/6 mice with/without lactic acid in low glucose (2 mM) condition for 72h. (n=6 independent experiments with each experiment containing technical replicates). (C-E) CD25^{hi} CD127⁻ FoxP3⁺ cells were induced using kit purified CD4⁺ CD25⁻ T cells obtained from PBMC of healthy donors with/without lactic acid for 6 days in low glucose condition in the presence of TGFβ; (C) Percentage of CD25^{hi} CD127⁻ FoxP3⁺ cells at endpoint (gating strategy in S3F, color of the dot indicates matched donors), (D) Percentage of live cells as frequency of respective parent population (gating strategy in S3G). (E) Division index after gating live cell populations for expression of CD4 and FoxP3 as indicated (gating strategy in S3F). (n=4 independent donors with each experiment containing technical replicates). (F-H) CD4⁺ CD25⁻ cells were purified using kit isolation from mice spleens and stimulated in low glucose condition for 72h with/without lactic acid and TGFβ. (F) Normalized mRNA expression of genes involved in the glycolytic pathway in CD4⁺ FoxP3^{RFP-} Tconv cells (teal) or CD4⁺ FoxP3^{RFP+} cells (pink), sorted after 72h stimulation in low glucose condition (n=2-3 biological replicates). (G) Glucose uptake measured by fold change in MFI of 2-NBDG (normalized to control group stimulated without TGFβ and lactic acid) of cells gated based on expression of FoxP3^{RFP} after 72h stimulation in low glucose condition (n=3 independent experiments). Error bars represent SD. (H) Seahorse measurements depicting baseline extracellular acidification rate (ECAR) of bulk iTregs induced in the presence of TGFβ for 72h in low glucose condition (n=3 independent experiments with at least three technical replicates within each experiment). Each dot is one independent experiment. pos (+); neg (-); Error bars represent SEM, unless otherwise stated. Statistical significance was determined

using one-way ANOVA followed by Sidak's multiple comparisons test (for A, D, E, G) or using two-tailed paired Student's t-test (for B, C, H). ns not significant, * *p*-value<0.05, ** *p*-value<0.01.

cells **(Fig S2C)**, without altered cell numbers **(Fig S2D)**, confirming an on-target effect of 2-DG. Next, we evaluated the effect of 2-DG on lactic acid-mediated conversion to FoxP3$^+$ cells. As earlier reported [30, 31], treatment with 2-DG during stimulation in the presence of TGFβ, reduced the frequency of FoxP3$^+$ cells **(Fig 2A)**, suggesting that glycolysis was essential for Treg induction. However, even in the presence of 2-DG, there was a persistent increase in the frequency of FoxP3$^+$ cells upon addition of lactic acid **(Fig 2A)**. Moreover, the increase in frequency was not due to a survival or a proliferative advantage of FoxP3$^+$ cells in the presence of lactic acid **(Fig S2E-F)**.

Our data indicated that lactic acid-mediated conversion to FoxP3$^+$ cells does not require high levels of glucose. Tregs with high glucose consumption are known to have reduced suppressive functions [16, 23]. Importantly, T cells often experience glucose limitation and high lactic acid levels at sites of inflammation and in the tumor [3, 12, 35]. Therefore, we combined these metabolically unfavorable conditions for further experiments. Glucose concentrations as low as 2 mM, did not impact the lactic acid-triggered increase in frequency **(Fig 2B)** and absolute counts **(Fig S3A)** of FoxP3$^+$ cells. Even in conditions of low glucose, we checked whether the increase in frequency of FoxP3$^+$ cells was due to a survival or a proliferative advantage in the presence of lactic acid. Interestingly there was a slight, but significant, increase in the viability of FoxP3$^-$ cells in the presence of lactic acid **(Fig S3B)**. There was no significant difference in the survival or proliferation of FoxP3$^+$ cells in the presence of lactic acid, in low glucose condition **(Fig S3B-C)**. We therefore concluded that there was an increased conversion to FoxP3$^+$ cells in the presence of lactic acid, also in low glucose conditions. Furthermore, there was a (non-significant) trend towards a dose-dependent increase in induction of FoxP3$^+$ cells in the presence of lactic acid, in low glucose condition **(Fig S3D)**. Increased frequencies of FoxP3$^+$ cells in the presence of lactic acid were consistently observed with Tconv cells that were purified using kit isolation **(Fig S3E)**, which in turn provided better cell yield, but slightly lower purity after isolation compared with sorted cells (data not shown). We therefore used kit isolation method for further experiments.

Next, we investigated whether our observations in the murine system are also detected in the human system. Importantly, there was a 3.2-fold increase in frequency of CD127$^-$ CD25^{hi}FoxP3$^+$ cells in the presence of lactic acid, using human CD4$^+$ CD25$^-$ T cells in low glucose conditions **(Fig 2C, S3F)**, indicating that the effect observed was not limited to murine T cells. We then tested whether FoxP3$^+$ cells have a survival or a proliferative advantage in the human setting. Presence of lactic acid did not impact the viability of either cell type **(Fig 2D, S3G)**. Evaluating the proliferation, there was a significant increase in proliferation of FoxP3$^+$ cells and a slight but insignificant increase in pro-

liferation of FoxP3$^-$ cells in the presence of lactic acid, compared to control condition without lactic acid **(Fig 2E, S3F)**. Taken together, our data indicated that lactic acid-mediated increase in FoxP3$^+$ cell frequency in low glucose condition occurred in both murine and human cells, but pointed towards potential species-specific regulation of FoxP3 induction and proliferation of cells.

Since the presence of extracellular lactic acid is known to reduce glycolysis in T cells [36], we set out to elucidate whether the tested dose of 10 mM lactic acid altered glycolysis in murine Tconv cells and FoxP3$^+$ cells after 72h induction in low glucose conditions. Confirming that the increase in low glucose and lactic acid-mediated Treg induction was present using cells isolated from spleen of FoxP3^{RFP} mice **(Fig S3H)**, allowed us to sort intact cells based on FoxP3^{RFP} expression for further analysis. To evaluate the glycolytic profile, we first investigated the mRNA expression of these cells, induced in low glucose condition with lactic acid. There were no differences in the expression of genes involved in the glycolytic pathway [16] of CD4$^+$ FoxP3^{RFP+} cells induced in the presence of lactic acid compared to control without lactic acid **(Fig 2F)**. This pattern was also observed for conventional CD4$^+$ FoxP3^{RFP-} cells that were stimulated without TGFβ **(Fig 2F)**, indicating that the tested dose of lactic acid did not alter glycolysis in CD4$^+$ T cells in low glucose conditions. Interestingly, FoxP3^{RFP+} cells showed reduced levels of Ldhb, involved in the conversion of lactate into pyruvate, and Slc16a1 (MCT1), one of the main lactate transporters, compared with FoxP3^{RFP-} cells, irrespective of lactic acid addition. In line with the RNA sequencing data, the glucose consumption, as measured by uptake of 2-NBDG, of either cell type was not altered upon stimulation in the presence of lactic acid **(Fig 2G)**. Next, we determined whether glycolysis remained intact upon stimulation of cells in low glucose condition in the presence of lactic acid using Seahorse analysis **(Fig 2H, S3I-K)**. There were no significant differences in glycolysis as measured by extracellular acidification rate (ECAR) **(Fig 2H)** or in mitochondrial respiration as measured by oxygen consumption rate (OCR) **(Fig S3I)**, of the bulk iTreg cells across conditions. Similar trends were observed in Tconv cells stimulated without TGFβ **(Fig S3J-K)**. Taken together, the observed increase in frequency of FoxP3$^+$ cells in low glucose condition, in the presence of lactic acid, was independent of their glycolytic profile.

FoxP3$^+$ cells induced in lactic acid and low glucose display a Treg-associated phenotype and function

We determined whether the FoxP3$^+$ cells induced with TGFβ, in the presence of lactic acid and low glucose indeed display characteristics of iTregs. The Treg signature [16] in cells sorted based on FoxP3^{RFP+} expression after 72h induction in the presence of lactic acid showed differences compared with control FoxP3^{RFP+} cells induced without lactic acid, in low glucose condition **(Fig 3A)**. We therefore evaluated the expression of Treg markers at protein level. There was no difference in the production of IL-10 **(Fig S4A)**

in the presence of lactic acid. Evaluating the surface marker expression, we observed a significant reduction in the expression of PD-1 **(Fig 3B-C)** and a slight (but insignificant) reduction in the expression of CCR4 **(Fig S4B-C)** while the expression of CD25, CTLA-4,

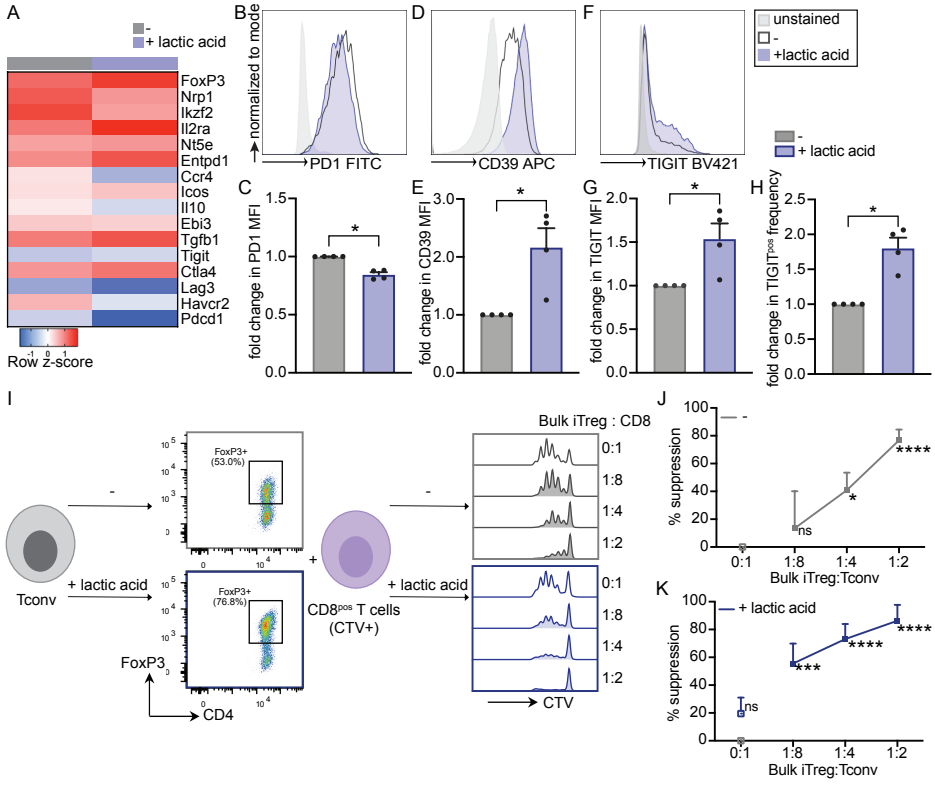

Fig 3: FoxP3⁺ cells induced in lactic acid and low glucose display a Treg-associated phenotype and function

(A) Normalized mRNA expression of Treg signature genes in CD4⁺ FoxP3^{RFP+} cells, sorted after 72h stimulation with TGFβ in low glucose (2 mM) condition with/without lactic acid (10 mM). (B-H) CD4⁺ CD25⁻ cells obtained from mice spleen were stimulated with TGFβ with/without lactic acid for 72h in low glucose condition and cells were gated for expression of FoxP3⁺ (gating strategy in S1A). Representative flow cytometry plots and fold change in MFI (normalized to untreated control cells induced without lactic acid) across experiments indicating expression of (B-C) PD-1, (D-E) CD39, (F-G) TIGIT on FoxP3⁺ cells and (H) fold change in frequency (normalized to untreated control cells induced without lactic acid) of TIGIT⁺ population within FoxP3⁺ cells (n=4 independent experiments with each experiment containing technical replicates). Error bars represent SEM and each dot is one independent experiment. (I) Set-up of suppression assay: CellTrace™ Violet (CTV) labelled CD8⁺ T cells were cultured with different ratios of bulk iTregs, induced in low glucose condition for 72h. Suppression assay was conducted in low glucose condition ± continuous presence of lactic acid. CTV plots indicates representative proliferation of CD8⁺ cells. Percent suppression was calculated using count of dividing cells after 72h coculture (gating strategy in S4J). (J-K) Percent suppression of CD8⁺ T cell proliferation by bulk iTreg induced in the (J) absence or (K) presence of lactic acid, measured by normalizing the number of proliferated cells to untreated CD8⁺ T cells control (n=3 independent experiments). Error bars represent SD. pos (+); neg (-); Statistical significance was determined using two-tailed unpaired Mann-Whitney U test (for C, E, G, H) or by comparing each group to untreated CD8⁺ T cells control using one-way ANOVA followed by Dunnett's multiple comparisons test (for J-K). ns not significant, * *p*-value<0.05, ** *p*-value<0.01, *** *p*-value<0.001, **** *p*-value<0.0001.

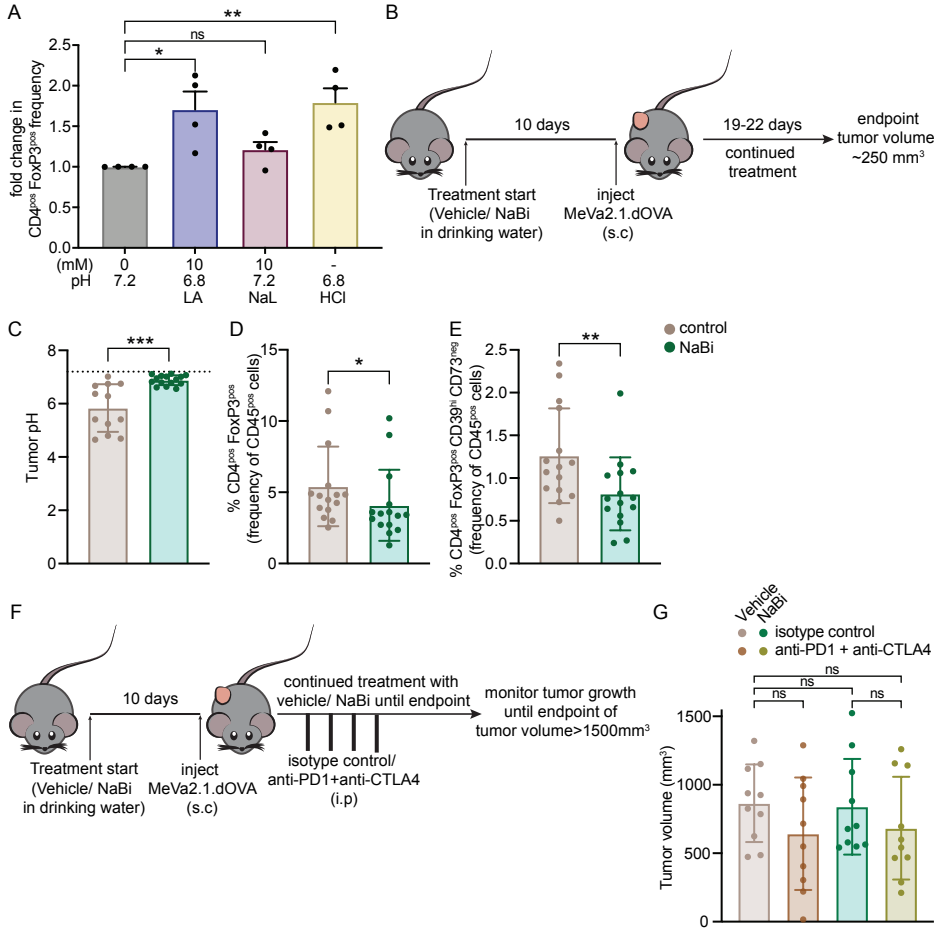

Fig 4: The effect of lactic acid on conversion to FoxP3⁺ cells is pH dependent

(A) Fold change (normalized to untreated control) in the frequency of FoxP3⁺ cells induced using sorted CD4⁺CD25⁻ Tconv cells obtained from spleens of C57BL/6 mice in the presence of lactic acid (LA) or sodium lactate (NaL) or media acidified with hydrochloric acid (HCl) for 72h (n=4 independent experiments with each experiment containing technical replicates). Each dot is one independent experiment and error bars represent SEM. (B-E) C57BL/6 mice were given NaBi (200 mM) or control drinking water for 10 days followed by sub-cutaneous (s.c) injection of MeVa2.1.dOVA tumor cells. Mice were terminated when the average tumor volume reached 250 mm³. (B) *in vivo* experiment setup to evaluate effect of NaBi on immune infiltration. (C) pH of tumor (n=12 in control and n=15 in NaBi treated mice) at endpoint (day 19 after tumor injection) across groups. Dotted line indicates average pH of blood in C57BL/6 mice. (D-E) Flow cytometry analysis indicating percentage of (D) CD4⁺ FoxP3⁺ cells and (E) CD4⁺ FoxP3⁺ CD39ʰⁱ CD73⁻ cells in the tumor of NaBi/vehicle treated MeVa2.1.dOVA bearing mice at endpoint (day 19 after tumor injection; n=15 per group; gating strategy in S5G). (F) *in vivo* experiment setup to evaluate tumor growth control: C57BL/6 mice were given NaBi (200 mM) or control drinking water for 10 days followed by s.c injection of MeVa2.1.dOVA tumor cells. When average tumor volume reached 100 mm³, mice received either anti-PD-1 (100 µg per dose per mouse) + anti-CTLA-4 (50 µg per dose per mouse) or the respective isotype controls (intra-peritoneal; two times per week for two weeks). Tumor growth was monitored until tumor volume was ≥ 1500 mm³. (G) MeVa2.1.dOVA tumor volume of mice treated with combinations of NaBi and anti-PD-1 + anti-CTLA-4 at the last timepoint at which all mice across all groups were alive (day 28 after tumor injection; n=10 mice per group). Each dot represents tumor from one mouse and error bars indicate SD, unless otherwise stated. pos

(+); neg (-); Statistical significance was determined by comparing each group to untreated control, using one-way ANOVA followed by Dunnett's multiple comparisons test (for A), or two-tailed unpaired Student's t-test (for C) or two-tailed unpaired Mann-Whitney U test (for D-E), or one-way ANOVA followed by Sidak's multiple comparisons test (for G). ns not significant, * *p*-value<0.05, ** *p*-value<0.01, *** *p*-value<0.001.

CD73 **(Fig S4D-I)** on FoxP3+ cells remained unaltered in the presence of lactic acid, in low glucose condition.

Interestingly, we observed a significant increase in the expression of the ecto-enzyme, CD39 on FoxP3+ cells induced in the presence of lactic acid, in low glucose condition **(Fig 3D-E)**. In addition, expression of TIGIT **(Fig 3F-G)** and the percentage of TIGIT+ cells **(Fig 3H)** were significantly higher in the presence of lactic acid.

To evaluate the functionality of FoxP3+ cells, we performed a co-culture of bulk iTregs with CTV labelled CD8+ T cells, in the continuous presence of lactic acid **(Fig 3I, S4J)**. The group without lactic acid was used as a control to ensure that it was possible to decipher the suppressive function of iTregs using this assay **(Fig 3J)**. Indeed, bulk iTregs induced in the presence of lactic acid and low glucose were capable of suppressing the proliferation of CD8+ T cells at different ratios **(Fig 3K)**. In summary, we established that the FoxP3+ cells expressed Treg-associated markers and exerted suppressive functions, despite being induced in metabolically unfavorable conditions.

The effect of lactic acid on conversion to FoxP3+ cells is pH-dependent

We observed reduced intracellular pH upon culturing cells in lactic acid **(Fig S5A)**, suggesting that acidification might impact the observed effect on increased conversion to FoxP3+ cells. We tested this by separating the impact of lactate and acidity in low glucose condition. Addition of sodium lactate (NaL) (pH neutral) did not lead to a significant increase in frequency of FoxP3+ cells **(Fig 4A)**. Notably, we observed that acidification of media with hydrochloric acid (HCl) alone was sufficient to recapitulate the observed increase in frequency of FoxP3+ cells in low glucose conditions **(Fig 4A)**. A latent form of TGFβ is present at low levels in media components used for culturing cells and acidity is known to cleave the latency-associated peptide (LAP) to release active TGFβ [37]. We also observed this in our complete cell culture media, wherein we detected active TGFβ upon acidification with HCl at pH 1 **(Fig S5B)**. However, the pH values obtained upon addition of lactic acid or HCl, at the doses used for induction (pH 6.8), were not sufficient to cleave LAP-TGFβ to produce its active form **(Fig S5B)**, ruling out that the effect observed on increased frequency of FoxP3+ cells was due to cleavage of latent TGFβ present in the culture media.

An advantage for Tregs in low pH is especially relevant in the context of the TME [5, 6]. Based on our *in vitro* evidence, we hypothesized that targeting tumor acidity might

alter Treg populations. Moreover, sodium bicarbonate (NaBi) administration via drinking water has been shown to reduce acidity in the tumor [38]. To evaluate the effect of altering tumor pH on Treg frequencies, we administered C57BL/6 mice with NaBi in drinking water followed by sub-cutaneous (s.c) injection of the syngeneic MeVa2.1.dOVA melanoma cell line [39] **(Fig 4B)**. We terminated the experiment at an average tumor volume of 250 mm^3, to avoid potential confounding factors, such as ulceration, necrosis, and hypoxia, which might be associated with larger tumor sizes. At this experimental endpoint, we first established that with an average pH of 5.4, the tumor was highly acidic compared with blood (average pH 7.2) **(Fig S5C)**. As expected [40], systemic NaBi administration to tumor-bearing mice did not alter the pH of blood, whereas the pH of urine was higher compared with the control group indicating clearance of excessive systemic bicarbonate **(Fig S5D-E)**. Importantly, NaBi administration significantly increased the average tumor pH up to 6.9 in these mice **(Fig 4C)**. There was no difference in the weight of MeVa2.1.dOVA tumors at the time of harvest in NaBi versus vehicle control treated mice **(Fig S5F)**. NaBi administration moderately, but significantly lowered the frequency of $FoxP3^+$ Tregs in the tumor compared to control animals **(Fig 4D, S5G)**, while the frequency of $FoxP3^-$ Tconv cells remained unaltered **(Fig S5H)**. There were no differences in the frequencies of total $CD8^+$ T cells in the tumor upon NaBi administration **(Fig S5G, S5I)**. The slight reduction in the frequency of Tregs was not sufficient to obtain a significant improvement in the $CD8^+$ T cells/Tregs ratio upon NaBi administration **(Fig S5J)**.

Moreover, our *in vitro* results showed a lactic acid-induced phenotype on iTregs characterized by increased expression of TIGIT and CD39, but no effect on the expression of CD73, which is often described to act in concert with CD39 [41]. We therefore evaluated the expression of these specific markers within the Treg populations *in vivo* by gating for the $CD39^{hi}$ $CD73^-$ subset **(Fig S5G)**. Importantly, in line with our *in vitro* findings, we observed a significant reduction in the frequency of $CD39^{hi}$ $CD73^-$ Tregs in the tumor upon increasing pH via NaBi treatment **(Fig 4E)**. Although we observed an elevated frequency of $TIGIT^+$ Tregs in the presence of lactic acid *in vitro*, these observations could not be recapitulated *in vivo* since there was no TIGIT expression on Tregs across any groups (data not shown).

We then examined whether NaBi administration either alone or in combination with immune checkpoint blockade results in tumor growth control in our model **(Fig 4F)**. NaBi administration had no impact on tumor volume at endpoint **(Fig 4G)**. While there was a slightly reduced tumor growth in groups treated with anti-PD-1 + anti-CTLA-4, this effect could not be further improved by NaBi administration **(Fig 4G, S5K)**. In summary, these results indicate that targeting tumor-associated acidity, using NaBi, lowers the frequency of Treg subsets in the tumor, but this was not sufficient to obtain tumor growth control in the MeVa2.1.dOVA model.

Discussion

The survival and suppressive functions of Tregs remain unaltered, or are even favored in lactic acid-rich environments, present in the TME [16, 17, 22]. However, it is not established whether the versatile metabolic profile of Tregs [18], which provides them with a functional advantage in the presence of lactic acid, also holds true in the context of Treg induction. We show here that the presence of extracellular lactic acid increased the conversion of Tconv cells to FoxP3$^+$ iTregs in a TGFβ-dependent manner, irrespective of glucose availability. Whereas a proliferative or survival advantage did not contribute to the observed increase in frequency of mouse FoxP3$^+$ cells, we observed differences in proliferation of human cells. Moreover, the magnitude of increase in frequency in low glucose condition was higher in the human compared to the murine setting (fold increase of 3.17 and 2.07, respectively), indicating that this could result from the proliferative advantage of human FoxP3$^+$ cells in the presence of lactic acid. Thus, future studies aiming to decipher molecular regulators of induction of FoxP3$^+$ cells in the presence of lactic acid should also take into account the potential species-specific effects.

The levels of lactic acid and glucose used in our *in vitro* setting have been previously described to occur in the TME [12, 42]. Whereas activation of CD4$^+$ T cells in metabolically unfavorable conditions results in anergy [34, 43], we show that FoxP3$^+$ cells induced in the presence of low glucose and lactic acid retained their suppressive function. In contrast to a recent report indicating lactic acid induced increased expression of PD-1 on effector Tregs (eTregs) [44], we observed a lower level of PD-1 in FoxP3$^+$ cells induced in the presence of low glucose and lactic acid. The former study showed that lactic acid uptake via monocarboxylate transporter 1 (MCT1) resulted in the observed increase in PD-1 expression on eTregs, and that this subset had a particularly high expression of MCT1 [44]. However, our RNA seq data showed a lower level of MCT1 (Slc16a1) in FoxP3$^+$ cells compared to FoxP3$^-$ cells in low glucose condition, irrespective of lactic acid addition, which might partially explain the observed differences between the two studies.

A high concentration of pH-neutral extracellular lactate has been shown to increase the frequency of murine iTregs mainly due to reduced proliferation of FoxP3$^-$ cells [22]. However, we did not observe a significant increase in the frequency of iTregs upon addition of sodium lactate, likely owing to the use of a lower dose of sodium lactate compared with the former study [22]. Likewise, we did not observe differences in proliferation of the murine FoxP3$^-$ T cell fraction or the FoxP3$^+$ fraction induced in the presence of lactic acid. However, lactic acid can alter proliferation of murine CD8$^+$ T cells at doses similar to those tested in our study [45]. This is due to the high glycolytic activity of CD8$^+$ T cells, therefore leading to the build-up of intracellular lactate [13]. This has recently been shown to occur in human CD4$^+$ T cells as well [34]. It is plausible that

there are slight species-related differences in sensitivity of CD4 T cells to lactic acid. Also, differences in stimulation conditions and glucose levels in the culture media between our study and the existing study [34], might impact the observed effect of lactic acid on $CD4^+$ T cell proliferation. As with the comparison between CD8 [13] and CD4 T cell subsets, our data indicated that the T cell subsets might differ in their sensitivity to the tested dose of lactic acid. Murine $CD4^+$ T cells are known to have lower glycolytic activity upon stimulation compared with $CD8^+$ T cells [46], which might explain the sustained proliferation in the presence of lactic acid in our study. In line with this, glycolysis was not impaired upon stimulating $CD4^+$ T cells in the presence of lactic acid in low glucose condition in our study.

Conversion of $CD4^+$ T cells to $FoxP3^+$ Tregs in the tumor is aided by several soluble factors (such as tumor antigens, TGFβ, IL-10, tumor derived extracellular vesicles) and the presence of specific immune cell types (such as Myeloid Derived Suppressor Cells) [20, 26, 27, 47–49]. Our data suggest that presence of lactic acid might be an additional factor involved in $FoxP3^+$ Treg induction in the tumor. Targeting tumor-associated acidity is known to reduce tumor growth by increasing the cytokine production by effector T cells [3, 14, 38, 50]. Here, we show that, this might have added benefits by reducing the frequency of $FoxP3^+$ Tregs in the tumor, thereby corroborating our *in vitro* findings. The reduced Treg frequencies in the tumor might in turn contribute to decreased Treg-mediated suppression, thus causing an increase in functionality of effector T cells. However, dissecting the effect of targeting acidity versus Tregs in the tumor, on functionality of effector T cells was beyond the scope of our study and is a limitation of our *in vivo* data.

Furthermore, we observed an increased expression of CD39 on iTregs induced in the presence of lactic acid. The presence of $CD39^+$ Tregs in the tumor is associated with increased suppressive functions [51, 52]. Correspondingly, blocking its activity results in tumor growth control in murine models of melanoma and fibrosarcoma [53]. CD39 and CD73 are known to liaise in the conversion of extracellular adenosine triphosphate (ATP) to adenosine, thereby exerting immune-suppressive effects [41]. Since we observed a lactic acid-mediated induction of CD39 expression, but not that of CD73 on iTregs *in vitro*, we evaluated the effect of altering tumor pH on the specific $CD39^{hi}CD73^-$ subset of Tregs, and observed a significant reduction of this subset upon NaBi administration. Moreover, expression of CD39 and its activity alone is sufficient to reduce the levels of extracellular ATP, thus reducing pro-inflammatory signals [53]. Therefore, it is likely that the $CD39^+CD73^-$ Treg subset is capable of exerting immune suppressive functions, which is then reduced by NaBi administration in our *in vivo* model.

While NaBi administration increased murine tumor pH, in line with earlier reports [38], there was no effect on tumor growth control, even in combination with anti-PD-1 + anti-CTLA-4. It has been previously shown that NaBi administration does not result in

tumor growth control in all melanoma models, despite causing a significant reduction in tumor associated acidity [38]. For example, in the B16 melanoma model, NaBi administration alone was not sufficient to control tumor growth. Also, NaBi in combination with dual checkpoint blockade of PD-1 and CTLA-4 did not result in an additive effect on tumor growth control compared with checkpoint blockade therapy [38]. Given our *in vivo* results, it is plausible that NaBi administration is insufficient to control tumor growth, at least in some melanoma models [38]. Moreover, we have previously shown that Treg depletion results in prolonged survival of MeVa2.1.dOVA tumor bearing mice [39]. However, NaBi administration did not result in a comparable reduction in Treg frequencies in the tumor as earlier observed with the Treg depleting anti-mouse CD25 antibody treatment [39]. Thus, we reasoned that the lack of a NaBi effect in our MeVa2.1.dOVA model might also arise from a relatively small therapeutic window for tumor growth control upon Treg depletion [39] compared with other models (such as CT26) that are amenable to growth control via targeting Tregs [54]. Additionally, not all the evaluated tumors in our study had pH values comparable to that of blood in NaBi-treated mice. Exploring other available agents to alter pH in the tumor such as proton pump inhibitors [14], or inhibiting MCT activity [7, 16], might further increase pH in the TME, in turn impacting Treg subsets and resulting in improved tumor growth control. It is tempting to speculate that the observed reduction in Treg frequency in the tumor might result in an additive effect on tumor growth control, upon combining buffering therapies with other treatment modalities, such as immune checkpoint blockade [16, 38], but this remains to be studied in other syngeneic murine tumor models.

Treg can utilize lactic acid as an alternative fuel source for both mitochondrial respiration (via conversion to pyruvate) and for glycolytic pathways (via conversion to phosphoenol pyruvate) in conditions of the TME [16]. However, we observed a lactate-independent effect, wherein acidity alone was sufficient to cause increased induction of Tregs. Moreover, sites of inflammation are associated with low pH, which might be caused by high immune cell activity [10, 11]. Extracellular acidosis can modulate the functionality of several immune cell types, resulting in stimulation or inhibition of innate immune responses and suppression of effector T cell-mediated immune responses [55]. Lactic acid is also known to induce M2-like functional polarization of tumor associated macrophages, thereby promoting tumor growth [56]. It is conceivable that, the acidity-mediated increase in Treg conversion during inflammation, evolved to facilitate immune resolution and tissue repair [57, 58], but such an effect becomes counter-productive in the context of the TME due to dampened anti-tumor immunity.

In conclusion, our study describes a previously unknown effect of acidity on Treg induction, which warrants further investigation in tumor models and models of inflammation.

Materials and methods

Mice and mice strains

C57BL/6JRj (C57BL/6) mice were purchased from Janvier. C57BL/6-*Foxp3*^{tm1Flv}/J (FoxP3^{RFP}) embryos were purchased from the Jackson Laboratory. FoxP3^{RFP} mice were then re-derived and homozygous mice were bred and maintained in the animal facility at the Netherlands Cancer Institute. All mice were housed under standard conditions with *ad libitum* access to food and drinking water. For *in vitro* experiments, spleens harvested from both male and/ or female mice, between the age of 8-16 weeks were used. For *in vivo* experiments, female mice at the age of 8 weeks were used. All animal experiments were performed in accordance with institutional and national guidelines and were approved by the Experimental Animal Committee of the Netherlands Cancer Institute.

Mouse T cell isolation and culture

Spleens were harvested from C57BL/6 or from FoxP3^{RFP} mice and mashed on a 70 μm cell strainer to obtain single cell suspension. After red blood cell (RBC) lysis using RBC lysis buffer (cat: 420301, BioLegend), CD4$^+$ T cells were isolated using Dynabeads™ Untouched™ mouse CD4 cell kit (cat: 11415D, ThermoFisher Scientific) as per manufacturer's instructions. To obtain Tconv cells, purified CD4$^+$ T cells were sorted by gating for live cells followed by positive expression of CD4 and negative expression of CD25 using FACSAria™ Fusion (BD Biosciences). Alternatively, Tconv cells were obtained directly from splenocytes after kit purification using mouse CD4$^+$ CD25$^+$ Regulatory T cell Isolation kit (cat: 130-091-041, Miltenyi Biotec), by collecting the negative fraction, containing CD4$^+$ CD25$^-$ cells. Cells were cultured in RPMI 1640 media (no glucose, cat: 11879020, ThermoFisher Scientific) supplemented with 10% heat inactivated Fetal Bovine Serum (HI-FBS) (cat: 3101517, Capricorn Scientific), penicillin-streptomycin (cat: 15140122, ThermoFisher Scientific), 50 IU/mL recombinant murine interleukin-2 (rmIL-2) (Cat: 12340026, ImmunoTools) and 50 μM 2-mercaptoethanol (Merck) (described as complete T cell culture media). For normal glucose condition, 10 mM D-Glucose (cat: G7021, Sigma-Aldrich) was added and for low glucose condition, 0.5 mM D-Glucose was added to culture media. The glucose level in the batches of HI-FBS used was approximately 1.5-2 mM, measured using Glucose Assay kit (cat: GAHK20, Sigma), as per manufacturer's instructions. Where relevant, cells were labelled with CellTrace™ Violet (CTV) (1.25 μM, cat: C34557, ThermoFisher Scientific) to track cell proliferation. Absolute counts of live cells were measured using CASY counter (Innovatis) or using Intellicyt® iQue Screener PLUS (Sartorius) flow cytometer. For measurement of absolute count using Intellicyt, cells across conditions were resuspended in the same volume of buffer and the entire sample was used for flow cytometry, therefore allowing cross-condition comparisons.

Mouse Treg induction

Sorted or kit purified Tconv cells were stimulated in the presence of plate-bound anti-mouse CD3 (1.25 μg/ml) (clone: 145-2C11, cat: 16003186, eBioscience™) and soluble anti-mouse CD28 (2.5 μg/ml) (clone: 37.51, cat: 16003185, eBioscience™) antibodies. Either 96-well ($5x10^4$ cells per well) or 24-well plates ($1x10^6$ cells per well) (non-tissue culture treated; Corning) were used. During stimulation, recombinant mouse Transforming Growth Factor-beta1 (TGFβ1) (3 ng/ml) (cat: 763102, BioLegend) was added to induce Tregs. Cell density and stimulation conditions were optimized to prevent acidification of the media at the endpoint in the control conditions due to cell proliferation, and to obtain consistent induction of Tregs. Where indicated, L-lactic acid (10 mM, unless otherwise stated) (cat: L1750, Sigma-Aldrich), sodium L-lactate (10 mM) (cat: L7022, Sigma-Aldrich), hydrochloric acid (HCl) (cat: 30721, Sigma-Aldrich), or 2-Deoxy-D-glucose (2-DG) (0.5 mM) (cat: D6134, Sigma-Aldrich), was added. Cells were incubated at 37 °C for 72h. At the endpoint, cells were harvested for further analyses.

Human PBMC isolation and Treg induction

Peripheral Blood Mononuclear Cells (PBMCs) were isolated from blood of healthy donors by density gradient separation using Ficoll (cat: 11743219, ThermoFisher Scientific). $CD4^+$ $CD25^-$ T cells were obtained from untouched fraction of cells isolated using Dynabeads™ Regulatory $CD4^+/CD25^+$ T Cell Kit (cat: 11363D, ThermoFisher Scientific) as per manufacturer's instructions. Cells were then stimulated using plate-bound anti-human CD3 (5 μg/ml) (clone: OKT3, cat: 15171506, ThermoFisher Scientific) and soluble anti-human CD28 (1 μg/ml) (clone:CD28.2, cat: 16028985, ThermoFisher Scientific) antibodies. In addition, for Treg induction, recombinant human TGFβ1 (5 ng/ml) (cat: 100-21, Peprotech) was added. Assay was set-up in RPMI media (no glucose) supplemented with 0.5 mM D-Glucose, 10% HI-FBS, penicillin-streptomycin, 100 IU/mL human interleukin-2 (Proleukin) and 50 μM 2-mercaptoethanol. 10 mM lactic acid was added to relevant conditions. Cells were incubated 37 °C for six days and then harvested for flow cytometry analysis.

Suppression assay

$CD8^+$ T cells were isolated from spleen of either C57BL/6 or $FoxP3^{RFP}$ mice using Dynabeads® Untouched™ Mouse CD8 Cells Kit (cat: 11417D, ThermoFisher Scientific) as per manufacturer's instructions. Purified $CD8^+$ T cells were then labelled with CTV to track cell proliferation. Assay was set-up in 96-well u-bottom plate, using $2.5x10^4$ $CD8^+$ T cells per well. For stimulation, soluble anti-mouse CD3 (1.25 μg/ml) was added. In addition, irradiated splenocytes (30 Gy, Gammacell® 40 Exactor) were added in the ratio of 1:1 to $CD8^+$ T cells. Bulk iTregs (cell pool containing $CD4^+$ $FoxP3^+$ and $CD4^+$ $FoxP3^-$ cells stimulated in the presence of TGFβ ± lactic acid) were harvested after 72h and co-cultured at different ratios, with CTV labelled $CD8^+$ T cells. Where indicated, lactic

acid was added. Cells were then cultured at 37 °C for 72h and then harvested for flow cytometry analysis to evaluate proliferation of $CD8^+$ T cells. To evaluate proliferating cells, dead cells were first excluded followed by gating for $CD8^+$ $CD4^-$ fraction. Cells were then gated for dilution of CTV. Percentage suppression was evaluated by counting the number of proliferating $CD8^+$ T cells using CTV dilution and normalizing to control condition containing $CD8^+$ T cells only (no lactic acid and no bulk iTregs).

***In vivo* experiments**

The MeVa2.1.dOVA tumor cell line [39] was cultured in DMEM/F-12 advanced medium (Cat: 12634028, ThermoFisher Scientific) supplemented with 10% HI-FBS, penicillin/streptomycin, and L-glutamine (cat: 25030024, ThermoFisher Scientific). Cells were regularly tested to be negative for mycoplasma. 8-week-old female C57BL/6 mice were administered with sodium bicarbonate (NaBi, 200 mM) (cat: S5761, Sigma-Aldrich) dissolved in the drinking water, and drinking water without NaBi was provided to control group. 10 days after treatment start, mice were injected sub-cutaneous (s.c) on the right flank with MeVa2.1.dOVA cell line (0.3 million cells), mixed with equal volume of matrigel (cat: 354234, Corning®). pH of urine was measured using pH indicator strips (cat: 1095330001, Sigma). For flow cytometry analysis, when the average tumor volume of both the groups reached 250 mm^3, mice were anesthetized (using isoflurane with oxygen) and tumor pH was measured using pH meter 5S (Sanxin). Where relevant, for pH measurement, blood was obtained under anesthesia, through heart puncture, using RAPIDLyte heparin coated syringes (cat: 08784181, Siemens) and pH was measured within 10 minutes of blood draw using RAPIDPoint® 500 blood gas analyzer (Siemens). After this, mice were terminated and tumors harvested for further analysis. For flow cytometry analysis, single cell suspensions of tumor tissues were obtained by mechanical disruption of the tissue by slicing, followed by 1h enzymatic digestion at 37 °C in medium containing 2 mg/mL collagenase A (cat: 11088793001, Roche) and 1 mg/mL DNAse (cat: 4716728001, Sigma-Aldrich). The suspension was filtered through a 70 μm cell strainer to remove debris.

Alternatively, for experiment to monitor tumor growth control, mice were pre-treated with NaBi for 10 days and injected with MeVa2.1.dOVA as described in the previous paragraph. Tumor volume was calculated using two-dimensional caliper measurements of the greatest longitudinal and transverse diameters: length × width x (width/2). When the average tumor volume was 100 mm^3, mice were randomized into treatment arms to receive either anti-PD-1 (100 μg/dose; clone RMP1-14, cat: BE0146) + anti-CTLA-4 (50 μg/dose; clone: 9D9, cat: BE0164) or their respective isotype controls (clone: 2A3, cat: BE0089 and clone: MPC-11, cat: BE0086, all purchased from BioXCell), intraperitoneal. Treatment with antibodies was given twice weekly for two weeks while NaBi administration continued throughout the entire duration of the study. Tumor growth was monitored until the endpoint tumor volume was ≥1500 mm^3. Alternatively, if mice

lost body weight (>15% compared to start of experiment), they were terminated before experimental endpoint.

Flow cytometry

Single cell suspension of tumor cells was obtained as described in the section of *in vivo* experiments. Alternatively, cells were harvested at endpoint of *in vitro* experiments. Fc blocking was performed using anti-mouse CD16/CD32 (cat: 14-0161-85, eBioscience™). This was followed by extracellular staining for cell surface markers. Dead cells were excluded using LIVE/DEAD™ fixable dead cell stain kit which stains dead cells (cat: L34968 or L34976, Invitrogen™). Where relevant, cells were then permeabilized using Intracellular Fixation & Permeabilization Buffer Set (cat: 00552100, eBioscience™) according to the manufacturer's protocol. This was followed by intracellular staining for FoxP3. Antibody details are listed in **Table 1**. Cells were finally suspended in flow cytometry buffer (2% HI-FBS in 1x phosphate buffered saline (PBS)) and acquired using LSR Fortessa™ (BD Biosciences) or Intellicyt® iQue Screener PLUS (Sartorius). Flow cytometry data analysis was performed using FlowJo (version 10.7.1, BD Life Sciences).

Table 1: List of antibodies used for flow cytometry analysis

Name	Clone	Conjugate (Catalogue number)	Manufacturer
Anti-mouse CD4	GK1.5	Brilliant Violet 785™ (100453)	BioLegend
Anti-mouse FoxP3	FJK-16s	APC (17-5773-82) PE (12-5773-82)	eBioscience™
Anti-mouse PD-1	J43	FITC (11-9985-85)	eBioscience™
Anti-mouse CD39	Duha59	APC (143809) PE/Dazzle™ 594 (143812)	BioLegend
Anti-mouse TIGIT	1G9	Brilliant Violet 421™ (142111)	BioLegend
Anti-mouse CD8	53-6.7	FITC (11-0081-85)	eBioscience™
Anti-mouse CCR4	2G12	APC (131211)	BioLegend
Anti-mouse CD25	PC61	PE (12-0251-83) Pacific Blue (102022)	eBioscience™ BioLegend
Anti-mouse CTLA-4	UC10-4B9	PE-Cyanine7 (106313)	BioLegend
Anti-mouse CD73	TY/11.8	FITC (127219) APC/Cyanine7 (127232)	BioLegend
Anti-mouse CD45.2	104	FITC (109806) PE-Cyanine7 (560696)	BioLegend BD Biosciences
Anti-human CD4	SK3	FITC (345768)	BD Biosciences
Anti-human CD25	M-A251	PE (560989)	BD Biosciences
Anti-human CD127	A019D5	Brilliant Violet 650™ (351325)	BioLegend
Anti-human FoxP3	236A/E7	APC (174777-41)	eBioscience™

Cytometric Bead Array

Supernatant was collected after stimulation of Tconv cells in Treg inducing conditions, as described in the section of mouse Treg induction, at the end of 72h incubation and snap frozen and stored at -20 °C until analysis. Cytometric Bead Array (CBA) to detect levels of IL-10 in the thawed supernatant was performed using Mouse IL-10 Flex Set (cat: 558300, BD Biosciences), as per manufacturer's instructions. Beads were acquired using Intellicyt® iQue Screener PLUS, and data analysis was performed using FlowJo. The levels of IL-10 in the supernatant were deduced from the standard curve.

ELISA

Lactic acid (10 mM) or HCl (pH equivalent volume) was added to complete T cell culture media (same composition as described in the section of mouse Treg induction). As positive control for acid activation of TGFβ present in the media components, complete T cell culture media was treated with 1N HCl followed by pH neutralization (using 1.2N NaOH/0.5M HEPES). Level of TGFβ across conditions was evaluated using Mouse TGF-beta 1 DuoSet ELISA kit (cat: DY1679, R&D Systems) as per manufacturer's instructions.

Glucose uptake assay

Glucose uptake of cells was measured across conditions after stimulation in the presence or absence of 2-DG (0.5 mM) for 72h. Alternatively, glucose uptake of cells was measured across conditions after stimulation in low glucose media for 72h. At the endpoint, cells were harvested, washed and stained with 2-deoxy-2-[(7-nitro-2,1,3-benzoxadiazol-4-yl) amino]-D-glucose (2-NBDG, 100 μg/ml diluted in media without glucose) (cat: 11046; Cayman Chemical). Cells were incubated for 30 minutes at 37 °C (lactic acid was continuously present in the relevant conditions) and then washed and finally suspended in flow cytometry buffer. Cells were acquired on LSR Fortessa™ (BD Biosciences) and intensity of 2-NBDG on the FITC channel was used to evaluate glucose uptake. Where mentioned, morphology of cells and FoxP3^{RFP} expression was used for pre-gating on respective cell types.

Seahorse analysis

At endpoint, either CD4$^+$ Tconv cells (stimulated without addition of TGFβ ± lactic acid) or bulk iTregs (cell pool containing CD4$^+$ FoxP3$^+$ and CD4$^+$ FoxP3$^-$ cells stimulated in the presence of TGFβ ± lactic acid) were harvested and media was replaced with low glucose Seahorse media (non-buffered RPMI (cat: R1383, Sigma-Aldrich) supplemented with 2 mM D-Glucose). Number of live cells were counted using CASY counter. 3x10^5 live cells per well were seeded in 100 μl in Cell-Tak (cat: 354240, Corning) coated XF24 plates (part of Seahorse XFe24 FluxPak, cat: 102340-100, Agilent Technologies) and allowed

to adhere for 30 minutes at 37 °C without CO_2. After this, 500 µl Seahorse media was added and cells were incubated for 15 minutes at 37 °C without CO_2. Oxygen consumption rate (OCR, pmol/min) and extracellular acidification rate (ECAR, mPh/min) were analyzed using Seahorse XFe24 metabolic analyzer (Agilent Technologies). Three to four baseline measurements were made per condition in each experiment. Wells containing media alone were used for background measurement.

Intracellular pH measurement

Bulk iTregs were loaded with 2',7'-bis-(2-Carboxyethyl)-5(6)-carboxyfluorescein acetoxymethyl ester (BCECF) AM (cat: B1150, ThermoFisher Scientific) staining solution (3.5 µM diluted in 1x PBS) and incubated at 37 °C for 30 minutes. Cells were then washed and resuspended in different media conditions ± lactic acid. Cells were then incubated at 37 °C for 20 minutes and harvested for flow cytometry analysis. Intracellular pH was calculated as per manufacturer's instructions using the BCECF staining intensity of samples and comparing with the generated standard curve using intracellular pH calibration buffer kit (cat: P35379, Invitrogen™).

RNA sequencing

Total RNA was isolated from cell pellets, using the RNeasy Mini Kit (Qiagen), including an on-column DNase digestion (Qiagen), according to the manufacturer's instructions. Quality and quantity of the total RNA was assessed by the 2100 Bioanalyzer using a Nano chip (Agilent, Santa Clara, CA). Total RNA samples having RIN>8 were subjected to library generation. Strand-specific libraries were generated using the TruSeq Stranded mRNA sample preparation kit (Illumina Inc.,) according to the manufacturer's instructions. Briefly, polyadenylated RNA from intact total RNA was purified using oligo-dT beads. Following purification, the RNA was fragmented, random primed and reverse transcribed using SuperScript II Reverse Transcriptase (Invitrogen) with the addition of Actinomycin D. Second strand synthesis was performed using Polymerase I and RNaseH with replacement of dTTP for dUTP. The generated cDNA fragments were 3' end adenylated and ligated to Illumina paired-end sequencing adapters and subsequently amplified by 12 cycles of PCR. The libraries were analyzed on a 2100 Bioanalyzer using a 7500 chip (Agilent), diluted and pooled equimolar into a multiplex sequencing pool. The libraries were sequenced with 65 base single reads on a HiSeq2500 using V4 chemistry (Illumina Inc.,). The samples were mapped with STAR (v2.7.3a) to mouse reference genome Mus_musulus.GRCm39.105 using default settings [59]. The read counts were computed with HTseq-count (v0.12.4) and were analyzed with DESeq2 (v1.30.1) [60]. Scaling of the normalized gene expression read counts was performed by subtracting the row means and scaling by dividing the columns by the standard deviation (SD) to generate a z-score. Heatmaps were generated from average z-score values of replicates using Graphpad Prism.

Statistical analyses

Statistical analyses were performed using Graphpad Prism (Graphpad Software Inc., v9). Two-tailed Student's t test or Mann-Whitney U test (for samples that did not follow Gaussian distribution) were used to compare means across two groups. Mean values across more than two groups were compared using one-way ANOVA followed by correcting for multiple comparisons using Sidak's test or Dunnett's test. The test used for each experiment is stated in the figure legend. *P*-value<0.05 was considered statistically significant.

Data availability

The RNA sequencing data included in this study has been deposited at GEO under the accession ID GSE217536 and will be available upon request.

Ethics approval

All the animal studies included in this manuscript have been conducted in accordance with the Dutch legislation and were approved by the Institutional Review Board at the Netherlands Cancer Institute.

Funding

Daniel S. Peeper was funded by Oncode Institute.

Acknowledgements

We thank the Flow Cytometry, Animal Laboratory, and Genomics core facilities, RHPC admin at Netherlands Cancer Institute for technical support. We thank all members of Blank and Peeper groups for scientific support and valuable feedback.

Author contributions

Disha Rao and Ruben Lacroix were involved in conceptualization of the study. Disha Rao, Ruben Lacroix, Kathrin Renner, Daniel S. Peeper and Christian U. Blank were involved in experiment design. Disha Rao, Johanna A. Stunnenberg, Joanna Kaplon, Fabienne Verburg, Paula T. van Royen and Esmée P. Hoefsmit were involved in the methodology, investigation and validation. Disha Rao and Petros Dimitriadis were involved in software and formal analysis. The original draft was written by Disha Rao, Christian U. Blank and Daniel S. Peeper. All authors were involved in the review and editing of the manuscript. Daniel S. Peeper and Christian U. Blank obtained funding and supervised the study.

Conflict of interests

Christian U. Blank declares the following potential conflict of interest: advisory roles for BMS, MSD, Roche, Novartis, GSK, AZ, Pfizer, Lilly, Genmab, Pierre Fabre, Third Rock Ventures, research funding from BMS, Novartis, NanoString, co-founder and shareholder of Immagene B.V. and Signature Oncology. Daniel S. Peeper is co-founder, shareholder and advisor of Immagene B.V., which is unrelated to this study. All other authors declare no conflict of interest.

References

1. Warburg O, Wind F, Negelein E. The metabolism of tumors in the body. J Gen Physiol. 1927 Mar;8(6):519–30.
2. Halestrap AP, Price NT. The proton-linked monocarboxylate transporter (MCT) family: structure, function and regulation. Biochem J. 1999 Oct;343 Pt 2(Pt 2):281–99.
3. Brand A, Singer K, Koehl GE, Kolitzus M, Schoenhammer G, Thiel A, Matos C, Bruss C, Klobuch S, Peter K, Kastenberger M, Bogdan C, Schleicher U, Mackensen A, Ullrich E, Fichtner-Feigl S, Kesselring R, Mack M, Ritter U, Schmid M, Blank C, Dettmer K, Oefner PJ, Hoffmann P, Walenta S, Geissler EK, Pouyssegur J, Villunger A, Steven A, Seliger B, Schreml S, Haferkamp S, Kohl E, Karrer S, Berneburg M, Herr W, Mueller-Klieser W, Renner K, Kreutz M. LDHA-Associated Lactic Acid Production Blunts Tumor Immunosurveillance by T and NK Cells. Cell Metab. 2016 Nov;24(5):657–71.
4. Gerweck LE, Seetharaman K. Cellular pH gradient in tumor versus normal tissue: potential exploitation for the treatment of cancer. Cancer Res. 1996 Mar;56(6):1194–8.
5. Longo DL, Bartoli A, Consolino L, Bardini P, Arena F, Schwaiger M, Aime S. In Vivo Imaging of Tumor Metabolism and Acidosis by Combining PET and MRI-CEST pH Imaging. Cancer Res. 2016 Nov;76(22):6463–70.
6. Gillies RJ, Raghunand N, Karczmar GS, Bhujwalla ZM. MRI of the tumor microenvironment. J Magn Reson Imaging. 2002 Oct;16(4):430–50.
7. Renner K, Bruss C, Schnell A, Koehl G, Becker HM, Fante M, Menevse AN, Kauer N, Blazquez R, Hacker L, Decking SM, Bohn T, Faerber S, Evert K, Aigle L, Amslinger S, Landa M, Krijgsman O, Rozeman EA, Brummer C, Siska PJ, Singer K, Pektor S, Miederer M, Peter K, Gottfried E, Herr W, Marchiq I, Pouyssegur J, Roush WR, Ong S, Warren S, Pukrop T, Beckhove P, Lang SA, Bopp T, Blank CU, Cleveland JL, Oefner PJ, Dettmer K, Selby M, Kreutz M. Restricting Glycolysis Preserves T Cell Effector Functions and Augments Checkpoint Therapy. Cell Rep. 2019 Oct;29(1):135-150.e9.
8. Palsson-McDermott EM, O'Neill LAJ. The Warburg effect then and now: From cancer to inflammatory diseases. BioEssays. 2013 Nov 1;35(11):965–73.
9. Huber V, Camisaschi C, Berzi A, Ferro S, Lugini L, Triulzi T, Tuccitto A, Tagliabue E, Castelli C, Rivoltini L. Cancer acidity: An ultimate frontier of tumor immune escape and a novel target of immunomodulation. Vol. 43, Seminars in Cancer Biology. Academic Press; 2017. p. 74–89.
10. Farr M, Garvey K, Bold AM, Kendall MJ, Bacon PA. Significance of the hydrogen ion concentration in synovial fluid in rheumatoid arthritis. Clin Exp Rheumatol. 1985;3(2):99–104.
11. Ricciardolo FLM, Gaston B, Hunt J. Acid stress in the pathology of asthma. J Allergy Clin Immunol. 2004 Apr 1;113(4):610–9.

12. Ho PC, Bihuniak JD, Macintyre AN, Staron M, Liu X, Amezquita R, Tsui YC, Cui G, Micevic G, Perales JC, Kleinstein SH, Abel ED, Insogna KL, Feske S, Locasale JW, Bosenberg MW, Rathmell JC, Kaech SM. Phosphoenolpyruvate Is a Metabolic Checkpoint of Anti-tumor T Cell Responses. Cell. 2015 Sep;162(6):1217–28.
13. Fischer K, Hoffmann P, Voelkl S, Meidenbauer N, Ammer J, Edinger M, Gottfried E, Schwarz S, Rothe G, Hoves S, Renner K, Timischl B, Mackensen A, Kunz-Schughart L, Andreesen R, Krause SW, Kreutz M. Inhibitory effect of tumor cell–derived lactic acid on human T cells. Blood. 2007 Jan 25;109(9):3812–9.
14. Calcinotto A, Filipazzi P, Grioni M, Iero M, De Milito A, Ricupito A, Cova A, Canese R, Jachetti E, Rossetti M, Huber V, Parmiani G, Generoso L, Santinami M, Borghi M, Fais S, Bellone M, Rivoltini L. Modulation of microenvironment acidity reverses anergy in human and murine tumor-infiltrating T lymphocytes. Cancer Res. 2012 Jun;72(11):2746–56.
15. Pucino V, Certo M, Bulusu V, Cucchi D, Goldmann K, Pontarini E, Haas R, Smith J, Headland SE, Blighe K, Ruscica M, Humby F, Lewis MJ, Kamphorst JJ, Bombardieri M, Pitzalis C, Mauro C. Lactate Buildup at the Site of Chronic Inflammation Promotes Disease by Inducing CD4(+) T Cell Metabolic Rewiring. Cell Metab. 2019 Dec;30(6):1055-1074.e8.
16. Watson MJ, Vignali PDA, Mullett SJ, Overacre-Delgoffe AE, Peralta RM, Grebinoski S, Menk A V, Rittenhouse NL, DePeaux K, Whetstone RD, Vignali DAA, Hand TW, Poholek AC, Morrison BM, Rothstein JD, Wendell SG, Delgoffe GM. Metabolic support of tumour-infiltrating regulatory T cells by lactic acid. Nature. 2021 Feb;
17. Wang H, Franco F, Tsui YC, Xie X, Trefny MP, Zappasodi R, Mohmood SR, Fernández-García J, Tsai CH, Schulze I, Picard F, Meylan E, Silverstein R, Goldberg I, Fendt SM, Wolchok JD, Merghoub T, Jandus C, Zippelius A, Ho PC. CD36-mediated metabolic adaptation supports regulatory T cell survival and function in tumors. Nat Immunol. 2020 Mar;21(3):298–308.
18. Rao D, Verburg F, Renner K, Peeper DS, Lacroix R, Blank CU. Metabolic profiles of regulatory T cells in the tumour microenvironment. Cancer Immunol Immunother. 2021;
19. Hori S, Nomura T, Sakaguchi S. Control of regulatory T cell development by the transcription factor Foxp3. Science. 2003 Feb;299(5609):1057–61.
20. Li C, Jiang P, Wei S, Xu X, Wang J. Regulatory T cells in tumor microenvironment: new mechanisms, potential therapeutic strategies and future prospects. Mol Cancer. 2020;19(1):116.
21. Shang B, Liu Y, Jiang SJ, Liu Y. Prognostic value of tumor-infiltrating FoxP3+ regulatory T cells in cancers: A systematic review and meta-analysis. Sci Rep. 2015 Oct;5.
22. Angelin A, Gil-de-Gómez L, Dahiya S, Jiao J, Guo L, Levine MH, Wang Z, Quinn WJ, Kopinski PK, Wang L, Akimova T, Liu Y, Bhatti TR, Han R, Laskin BL, Baur JA, Blair IA, Wallace DC, Hancock WW, Beier UH. Foxp3 Reprograms T Cell Metabolism to Function in Low-Glucose, High-Lactate Environments. Cell Metab. 2017 Jun;25(6):1282-1293.e7.
23. Gerriets VA, Kishton RJ, Johnson MO, Cohen S, Siska PJ, Nichols AG, Warmoes MO, De Cubas AA, MacIver NJ, Locasale JW, Turka LA, Wells AD, Rathmell JC. Foxp3 and Toll-like receptor signaling balance T reg cell anabolic metabolism for suppression. Nat Immunol. 2016 Dec;17(12):1459–66.
24. Weinberg SE, Singer BD, Steinert EM, Martinez CA, Mehta MM, Martínez-Reyes I, Gao P, Helmin KA, Abdala-Valencia H, Sena LA, Schumacker PT, Turka LA, Chandel NS. Mitochondrial complex III is essential for suppressive function of regulatory T cells. Nature. 2019;565(7740):495–9.
25. Kishore M, Cheung KCP, Fu H, Bonacina F, Wang G, Coe D, Ward EJ, Colamatteo A, Jangani M, Baragetti A, Matarese G, Smith DM, Haas R, Mauro C, Wraith DC, Okkenhaug K, Catapano AL, De Rosa V, Norata GD, Marelli-Berg FM. Regulatory T Cell Migration Is Dependent on Glucokinase-Mediated Glycolysis. Immunity. 2017 Nov 21;47(5):875-889.e10.
26. Zhou G, Levitsky HI. Natural Regulatory T Cells and De Novo-Induced Regulatory T Cells Contribute Independently to Tumor-Specific Tolerance. J Immunol. 2007 Feb;178(4):2155–62.

27. Moo-Young TA, Larson JW, Belt BA, Tan MC, Hawkins WG, Eberlein TJ, Goedegebuure PS, Linehan DC. Tumor-derived TGF-beta mediates conversion of CD4+Foxp3+ regulatory T cells in a murine model of pancreas cancer. J Immunother. 2009 Jan;32(1):12–21.
28. Stephan S, Ludovica B, Arnulf H, David F, Marion L, Mikhail S, A. KZ, S. CB, Doreen C, Eric O, M. SK, G. FA, Matthias M. T cell receptor signaling controls Foxp3 expression via PI3K, Akt, and mTOR. Proc Natl Acad Sci. 2008 Jun 3;105(22):7797–802.
29. Chapman NM, Boothby MR, Chi H. Metabolic coordination of T cell quiescence and activation. Nat Rev Immunol. 2020;20(1):55–70.
30. Tanimine N, Germana SK, Fan M, Hippen K, Blazar BR, Markmann JF, Turka LA, Priyadharshini B. Differential effects of 2-deoxy-D-glucose on in vitro expanded human regulatory T cell subsets. PLoS One. 2019;14(6):e0217761.
31. De Rosa V, Galgani M, Porcellini A, Colamatteo A, Santopaolo M, Zuchegna C, Romano A, De Simone S, Procaccini C, La Rocca C, Carrieri PB, Maniscalco GT, Salvetti M, Buscarinu MC, Franzese A, Mozzillo E, La Cava A, Matarese G. Glycolysis controls the induction of human regulatory T cells by modulating the expression of FOXP3 exon 2 splicing variants. Nat Immunol. 2015;16(11):1174–84.
32. Lacroix R, Rozeman EA, Kreutz M, Renner K, Blank CU. Targeting tumor-associated acidity in cancer immunotherapy. Cancer Immunol Immunother. 2018;67(9):1331–48.
33. Chen W, Jin W, Hardegen N, Lei KJ, Li L, Marinos N, McGrady G, Wahl SM. Conversion of peripheral CD4+CD25- naive T cells to CD4+CD25+ regulatory T cells by TGF-beta induction of transcription factor Foxp3. J Exp Med. 2003 Dec;198(12):1875–86.
34. Decking SM, Bruss C, Babl N, Bittner S, Klobuch S, Thomas S, Feuerer M, Hoffmann P, Dettmer K, Oefner PJ, Renner K, Kreutz M. LDHB Overexpression Can Partially Overcome T Cell Inhibition by Lactic Acid. Int J Mol Sci. 2022 May;23(11).
35. de Oliveira PG, Farinon M, Sanchez-Lopez E, Miyamoto S, Guma M. Fibroblast-Like Synoviocytes Glucose Metabolism as a Therapeutic Target in Rheumatoid Arthritis. Front Immunol. 2019;10.
36. Wu H, Estrella V, Beatty M, Abrahams D, El-Kenawi A, Russell S, Ibrahim-Hashim A, Longo DL, Reshetnyak YK, Moshnikova A, Andreev OA, Luddy K, Damaghi M, Kodumudi K, Pillai SR, Enriquez-Navas P, Pilon-Thomas S, Swietach P, Gillies RJ. T-cells produce acidic niches in lymph nodes to suppress their own effector functions. Nat Commun. 2020;11(1):4113.
37. Oida T, Weiner HL. Depletion of TGF-β from fetal bovine serum. J Immunol Methods. 2010 Oct;362(1–2):195–8.
38. Pilon-Thomas S, Kodumudi KN, El-Kenawi AE, Russell S, Weber AM, Luddy K, Damaghi M, Wojtkowiak JW, Mulé JJ, Ibrahim-Hashim A, Gillies RJ. Neutralization of Tumor Acidity Improves Antitumor Responses to Immunotherapy. Cancer Res. 2016 Mar;76(6):1381–90.
39. Rao D, Lacroix R, Rooker A, Gomes T, Stunnenberg JA, Valenti M, Dimitriadis P, Lin CP, de Bruijn B, Krijgsman O, Ligtenberg MA, Peeper DS, Blank CU. MeVa2.1.dOVA and MeVa2.2.dOVA: two novel BRAFV600E-driven mouse melanoma cell lines to study tumor immune resistance. Melanoma Res. 2023;Feb 1(33(1)):12–26.
40. Robey IF, Nesbit LA. Investigating mechanisms of alkalinization for reducing primary breast tumor invasion. Biomed Res Int. 2013;2013:485196.
41. Deaglio S, Dwyer KM, Gao W, Friedman D, Usheva A, Erat A, Chen JF, Enjyoji K, Linden J, Oukka M, Kuchroo VK, Strom TB, Robson SC. Adenosine generation catalyzed by CD39 and CD73 expressed on regulatory T cells mediates immune suppression . J Exp Med. 2007 May 14;204(6):1257–65.
42. Sullivan MR, Danai L V, Lewis CA, Chan SH, Gui DY, Kunchok T, Dennstedt EA, Vander Heiden MG, Muir A. Quantification of microenvironmental metabolites in murine cancers reveals determinants of tumor nutrient availability. Elife. 2019 Apr;8.
43. Zheng Y, Delgoffe GM, Meyer CF, Chan W, Powell JD. Anergic T cells are metabolically anergic. J Immunol. 2009 Nov;183(10):6095–101.

44. Kumagai S, Koyama S, Itahashi K, Tanegashima T, Lin YT, Togashi Y, Kamada T, Irie T, Okumura G, Kono H, Ito D, Fujii R, Watanabe S, Sai A, Fukuoka S, Sugiyama E, Watanabe G, Owari T, Nishinakamura H, Sugiyama D, Maeda Y, Kawazoe A, Yukami H, Chida K, Ohara Y, Yoshida T, Shinno Y, Takeyasu Y, Shirasawa M, Nakama K, Aokage K, Suzuki J, Ishii G, Kuwata T, Sakamoto N, Kawazu M, Ueno T, Mori T, Yamazaki N, Tsuboi M, Yatabe Y, Kinoshita T, Doi T, Shitara K, Mano H, Nishikawa H. Lactic acid promotes PD-1 expression in regulatory T cells in highly glycolytic tumor microenvironments. Cancer Cell. 2022 Feb;40(2):201-218.e9.
45. Quinn WJ 3rd, Jiao J, TeSlaa T, Stadanlick J, Wang Z, Wang L, Akimova T, Angelin A, Schäfer PM, Cully MD, Perry C, Kopinski PK, Guo L, Blair IA, Ghanem LR, Leibowitz MS, Hancock WW, Moon EK, Levine MH, Eruslanov EB, Wallace DC, Baur JA, Beier UH. Lactate Limits T Cell Proliferation via the NAD(H) Redox State. Cell Rep. 2020 Dec;33(11):108500.
46. Cao Y, Rathmell JC, Macintyre AN. Metabolic Reprogramming towards Aerobic Glycolysis Correlates with Greater Proliferative Ability and Resistance to Metabolic Inhibition in CD8 versus CD4 T Cells. PLoS One. 2014 Aug 4;9(8):e104104.
47. Szajnik M, Czystowska M, Szczepanski MJ, Mandapathil M, Whiteside TL. Tumor-derived microvesicles induce, expand and up-regulate biological activities of human regulatory T cells (Treg). PLoS One. 2010 Jul;5(7):e11469.
48. Liu VC, Wong LY, Jang T, Shah AH, Park I, Yang X, Zhang Q, Lonning S, Teicher BA, Lee C. Tumor Evasion of the Immune System by Converting CD4+CD25− T Cells into CD4+CD25+ T Regulatory Cells: Role of Tumor-Derived TGF-β. J Immunol. 2007 Mar 1;178(5):2883 LP – 2892.
49. Paluskievicz CM, Cao X, Abdi R, Zheng P, Liu Y, Bromberg JS. T Regulatory Cells and Priming the Suppressive Tumor Microenvironment. Front Immunol. 2019;10:2453.
50. Uhl FM, Chen S, O'Sullivan D, Edwards-Hicks J, Richter G, Haring E, Andrieux G, Halbach S, Apostolova P, Büscher J, Duquesne S, Melchinger W, Sauer B, Shoumariyeh K, Schmitt-Graeff A, Kreutz M, Lübbert M, Duyster J, Brummer T, Boerries M, Madl T, Blazar BR, Groß O, Pearce EL, Zeiser R. Metabolic reprogramming of donor T cells enhances graft-versus-leukemia effects in mice and humans. Sci Transl Med. 2020 Oct;12(567).
51. Maj T, Wang W, Crespo J, Zhang H, Wang W, Wei S, Zhao L, Vatan L, Shao I, Szeliga W, Lyssiotis C, Liu JR, Kryczek I, Zou W. Oxidative stress controls regulatory T cell apoptosis and suppressor activity and PD-L1-blockade resistance in tumor. Nat Immunol. 2017 Nov;18(12):1332–41.
52. Ahlmanner F, Sundström P, Akeus P, Eklöf J, Börjesson L, Gustavsson B, Lindskog EB, Raghavan S, Quiding-Järbrink M. CD39(+) regulatory T cells accumulate in colon adenocarcinomas and display markers of increased suppressive function. Oncotarget. 2018 Dec;9(97):36993–7007.
53. Perrot I, Michaud HA, Giraudon-Paoli M, Augier S, Docquier A, Gros L, Courtois R, Déjou C, Jecko D, Becquart O, Rispaud-Blanc H, Gauthier L, Rossi B, Chanteux S, Gourdin N, Amigues B, Roussel A, Bensussan A, Eliaou JF, Bastid J, Romagné F, Morel Y, Narni-Mancinelli E, Vivier E, Paturel C, Bonnefoy N. Blocking Antibodies Targeting the CD39/CD73 Immunosuppressive Pathway Unleash Immune Responses in Combination Cancer Therapies. Cell Rep. 2019 May 21;27(8):2411-2425.e9.
54. Arce Vargas F, Furness AJS, Solomon I, Joshi K, Mekkaoui L, Lesko MH, Miranda Rota E, Dahan R, Georgiou A, Sledzinska A, Ben Aissa A, Franz D, Werner Sunderland M, Wong YNS, Henry JY, O'Brien T, Nicol D, Challacombe B, Beers SA, Consortium MTracer, Consortium RTracer, Consortium LTracer, Turajlic S, Gore M, Larkin J, Swanton C, Chester KA, Pule M, Ravetch J V, Marafioti T, Peggs KS, Quezada SA. Fc-Optimized Anti-CD25 Depletes Tumor-Infiltrating Regulatory T Cells and Synergizes with PD-1 Blockade to Eradicate Established Tumors. Immunity. 2017/04/11. 2017 Apr 18;46(4):577–86.
55. Erra Díaz F, Dantas E, Geffner J. Unravelling the Interplay between Extracellular Acidosis and Immune Cells. Granucci F, editor. Mediators Inflamm. 2018;2018:1218297.

56. Colegio OR, Chu NQ, Szabo AL, Chu T, Rhebergen AM, Jairam V, Cyrus N, Brokowski CE, Eisenbarth SC, Phillips GM, Cline GW, Phillips AJ, Medzhitov R. Functional polarization of tumour-associated macrophages by tumour-derived lactic acid. Nature. 2014 Sep;513(7519):559–63.
57. Li J, Tan J, Martino MM, Lui KO. Regulatory T-Cells: Potential Regulator of Tissue Repair and Regeneration. Vol. 9, Frontiers in Immunology. 2018.
58. Proto JD, Doran AC, Gusarova G, Yurdagul Jr. A, Sozen E, Subramanian M, Islam MN, Rymond CC, Du J, Hook J, Kuriakose G, Bhattacharya J, Tabas I. Regulatory T Cells Promote Macrophage Efferocytosis during Inflammation Resolution. Immunity. 2018 Oct 16;49(4):666-677.e6.
59. Dobin A, Davis CA, Schlesinger F, Drenkow J, Zaleski C, Jha S, Batut P, Chaisson M, Gingeras TR. STAR: ultrafast universal RNA-seq aligner. Bioinformatics. 2013 Jan;29(1):15–21.
60. Anders S, Pyl PT, Huber W. HTSeq—a Python framework to work with high-throughput sequencing data. Bioinformatics. 2015 Jan 15;31(2):166–9.

Supplemental figures

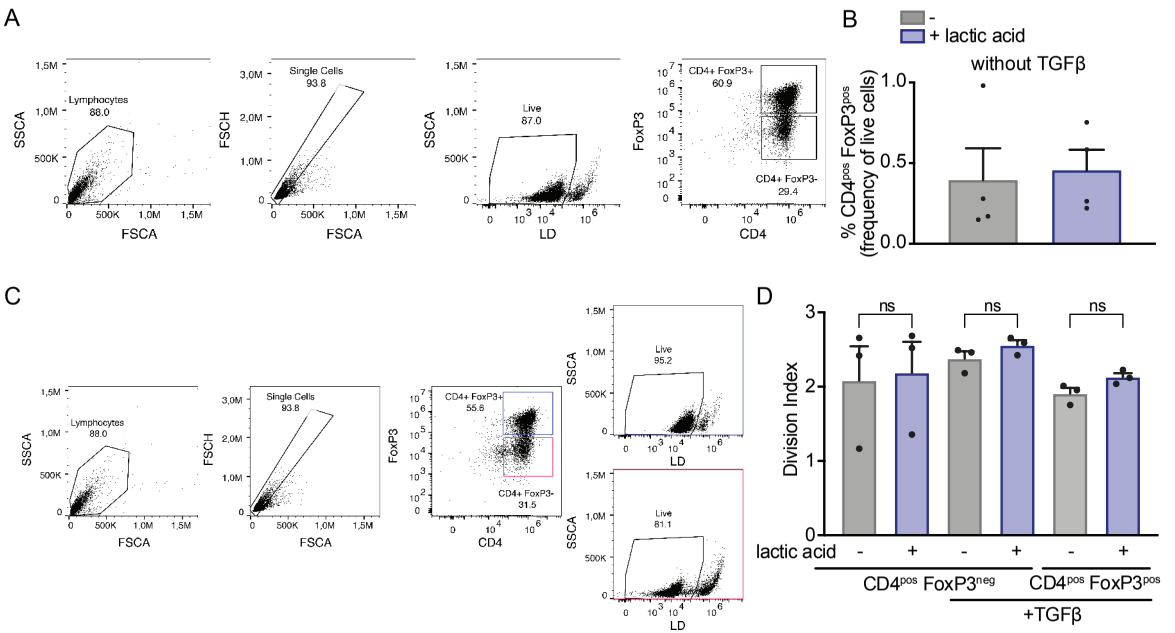

Fig S1 (supplement to figure 1): Increased induction of FoxP3$^+$ cells in the presence of lactic acid

(A) Gating strategy: Lymphocytes were gated based on forward and side scatter followed by doublet exclusion. This was followed by dead cell exclusion based on staining for dead cell stain (LD) and then by gating based on expression of CD4 and FoxP3. Numbers below the gate label indicate frequencies of parent population. (B) Percentage of FoxP3$^+$ cells after 72h stimulation without TGFβ (n=4 independent experiments with each experiment containing technical replicates). (C) Gating strategy to evaluate live cell percentages: Lymphocytes were gated based on scatter followed by doublet exclusion and then gated for expression of CD4 and FoxP3. Within each FoxP3$^+$ (blue) and FoxP3$^-$ (red) subsets, dead cells were excluded using dead cell staining dye (LD). Numbers below the gate label indicate frequencies of parent population. (D) Quantification of CellTrace^{TM} Violet indicating division index after gating live cell populations for expression of CD4 and FoxP3 as indicated after stimulation for 72h (n=3 independent experiments with each experiment containing technical replicates). Each dot is one independent experiment. pos (+); neg (-); Error bars represent SEM. Statistical significance was determined using one-way ANOVA followed by Sidak's multiple comparisons test (for D). ns not significant.

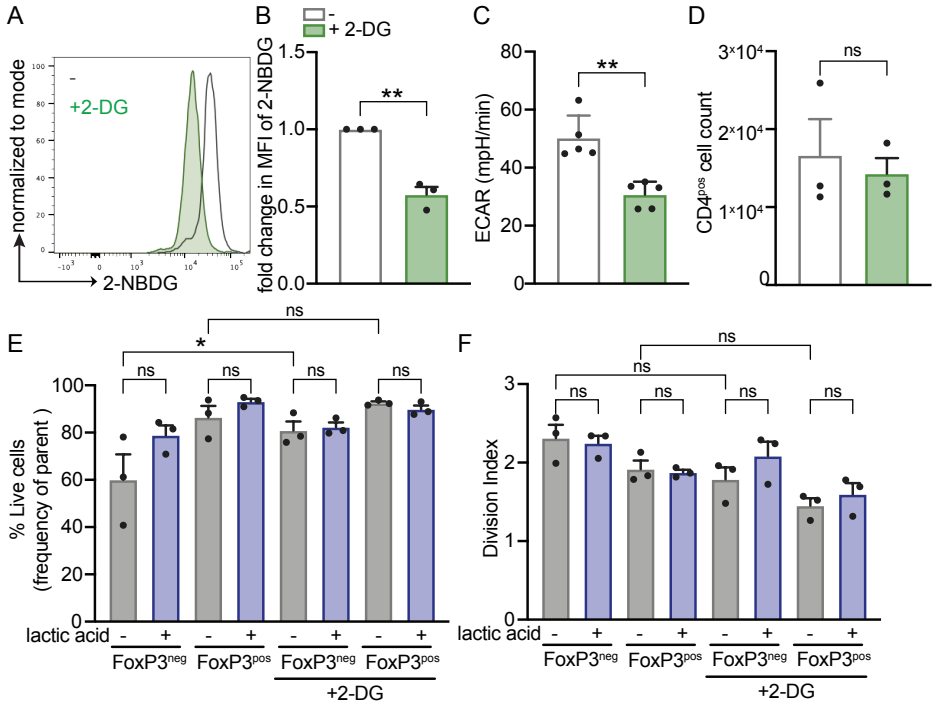

Fig S2 (supplement to figure 2): Lactic acid-mediated increase in FoxP3⁺ cells is independent of their glycolytic profile

(A-D) CD4⁺ T cells obtained from mice spleens were stimulated without TGFβ for 72h in normal glucose condition in the presence of 2-DG. (A) Representative histogram of 2-NBDG indicating glucose uptake and (B) fold change in MFI (normalized to untreated control) of 2-NBDG of CD4⁺ T cells (n=3 independent experiments with each experiment in technical replicates). (C) Seahorse analysis indicating baseline extracellular acidification rate (ECAR) (four measurements each of n=5 technical replicates). Error bars represent SD. (D) Count of CD4⁺ T cells, measured using Intellicyt (n=3 independent experiments with each experiment containing technical replicates). (E-F) Sorted CD4⁺ CD25⁻ Tconv cells obtained from spleens of C57BL/6 mice were stimulated with TGFβ ± 2-DG for 72h in normal glucose condition. (E) Percentage of live cells as frequency of respective parent population (gating strategy as in S1C) and (F) division index of indicated population (gating strategy as in S1A) (n=3 independent experiments with each experiment containing technical replicates). Each dot is one independent experiment. pos (+); neg (-); Error bars represent SEM, unless otherwise stated. Statistical significance was determined using two-tailed unpaired Student's t-test (for B) or by two-tailed paired Student's t-test (for C-D) or by one-way ANOVA followed by Sidak's multiple comparisons test (for E-F). ns not significant, * *p*-value<0.05, ** *p*-value<0.01.

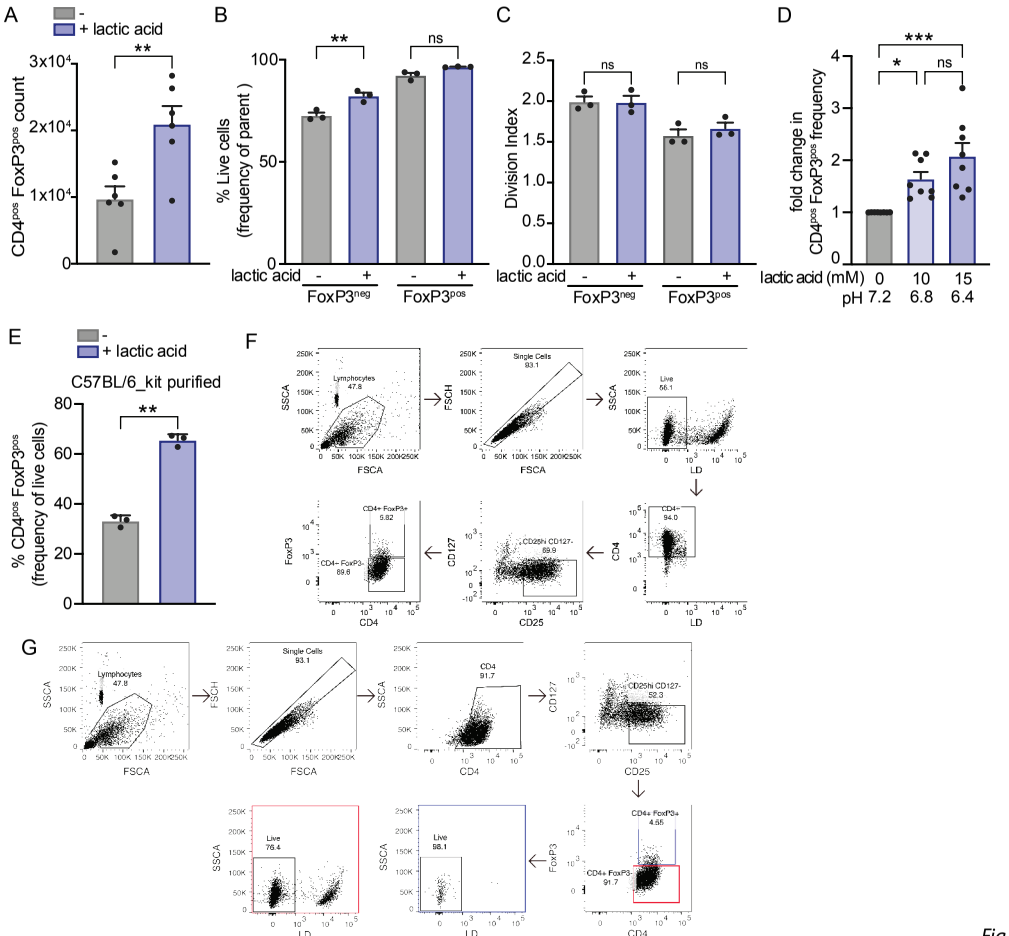

Fig S3 continues on next page.

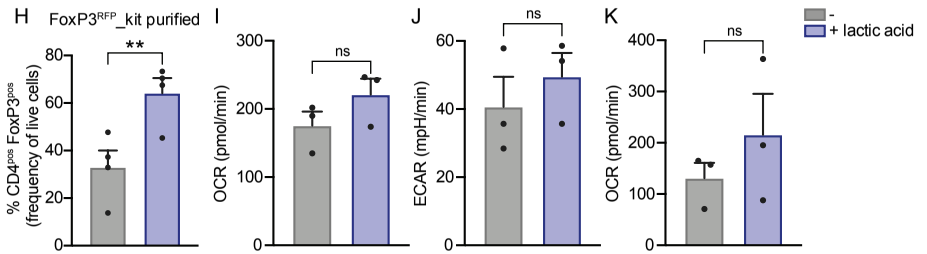

Fig S3 (supplement to figure 2): Lactic acid-mediated increase in FoxP3⁺ cells is independent of their glycolytic profile

(A-D) Sorted CD4⁺ CD25⁻ Tconv cells obtained from spleens of C57BL/6 mice were stimulated with TGFβ in the presence of lactic acid in low glucose condition for 72h. (A) Count of FoxP3⁺ cells at endpoint, measured using Intellicyt (n=6 independent experiments with each experiment containing technical replicates). (B) Percentage of live cells as frequency of respective parent population (gating strategy as in S1C) and (C) division index of indicated population (gating strategy as in S1A) (n=3 independent experiments with each experiment containing technical replicates). (D) Fold change in the frequency (normalized to untreated control) of FoxP3⁺ cells induced in the presence of different doses of lactic acid for 72h (n=8 independent experiments with each experiment containing technical replicates). (E) Percentage of CD4⁺ FoxP3⁺ cells obtained using kit purified CD4⁺ CD25⁻ Tconv cells isolated from spleens of C57BL/6 mice in low glucose condition (n=3 technical replicates; error bars are SD). (F) Gating strategy for human cells: Lymphocytes were gated based on scatter followed by doublet exclusion. This was followed by dead cell exclusion using dead cell stain (LD) and then by gating based on expression of CD4, CD25 and CD127. FoxP3 expression within the subset was then determined. Numbers below the gate label indicate frequencies of parent population. (G) Gating strategy to evaluate human live cell frequencies: Lymphocytes were gated based on scatter followed by doublet exclusion and then gated for expression of CD4, CD25 and CD127. FoxP3 expression in this subset was gated. Within each FoxP3⁺ (blue) and FoxP3⁻ (red) subsets, live cells were gated based on dead cell exclusion. Numbers below the gate label indicate frequencies of parent population. (H) Frequency of CD4⁺ FoxP3⁺ cells obtained using kit purified CD4⁺ CD25⁻ Tconv cells isolated from spleens of FoxP3^{RFP} mice in low glucose condition (n=4 independent experiments with at least two technical replicates within each experiment). (I-K) Seahorse measurements depicting baseline (I) oxygen consumption rate (OCR) of murine bulk iTregs induced with TGFβ for 72h in low glucose condition; (J) ECAR and (K) OCR of murine conventional CD4⁺ T cells stimulated without TGFβ for 72h in low glucose condition ± lactic acid. (n=3 independent experiments with at least three technical replicates within each experiment). Each dot is one independent experiment. pos (+); neg (-); Error bars represent SEM, unless otherwise stated. Statistical significance was determined using two-tailed paired Student's t-test (for A, E, H-K) or by one-way ANOVA followed by Sidak's multiple comparisons test (for B-D). ns not significant, * *p*-value<0.05, ** *p*-value<0.01, *** *p*-value<0.001.

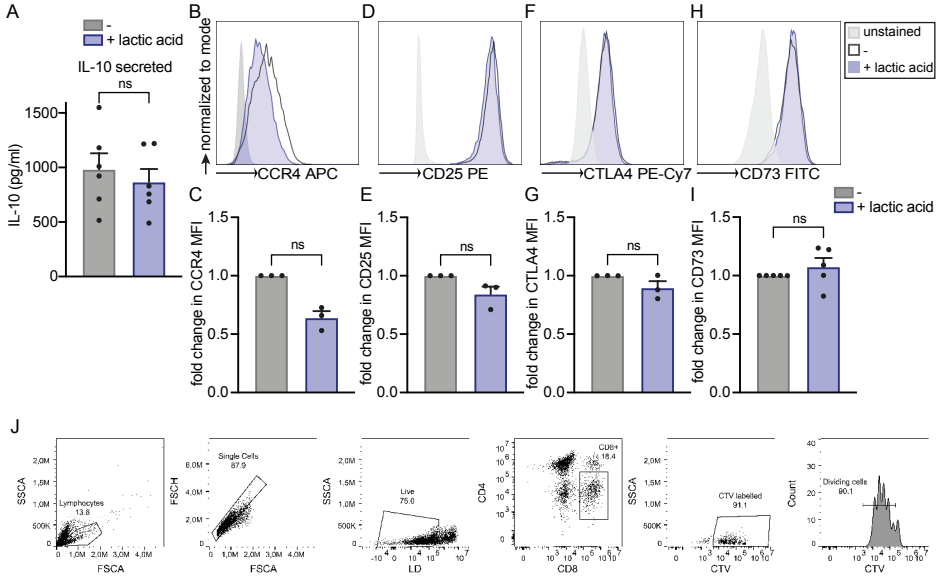

Fig S4 (supplement to figure 3): FoxP3$^+$ cells induced in lactic acid and low glucose display a Treg-associated phenotype and function

(A-I) CD4$^+$ CD25$^-$ cells obtained from mice spleens were stimulated in the presence of TGFβ ± lactic acid in low glucose condition for 72h. (A) secreted IL-10 in the supernatant of bulk iTregs induced in the presence of lactic acid in low glucose condition for 72h (n=6 independent experiments). (B-I) Representative flow cytometry plots and fold change in MFI (normalized to untreated control cells induced without lactic acid) indicating expression of (B-C) CCR4, (D-E) CD25, (F-G) CTLA-4 and (H-I) CD73 on FoxP3$^+$ cells (n=at least 3 independent experiments). (J) Gating strategy for suppression assay: Cells were first gated based on side scatter followed by doublet exclusion. This was followed by excluding dead cells and then selecting cells positive for CD8 expression and negative for CD4 expression. CD8 cells were then gated for labelling of CellTrace™ Violet followed by selecting dividing cells using histogram. Count of dividing cells, as measured by Intellicyt, was used for calculating percent suppression. Each dot is one independent experiment. Error bars represent SEM. Statistical significance was determined using two-tailed paired Student's t-test (for A) or using two-tailed unpaired Mann-Whitney U test (for C, E, G, I). ns not significant.

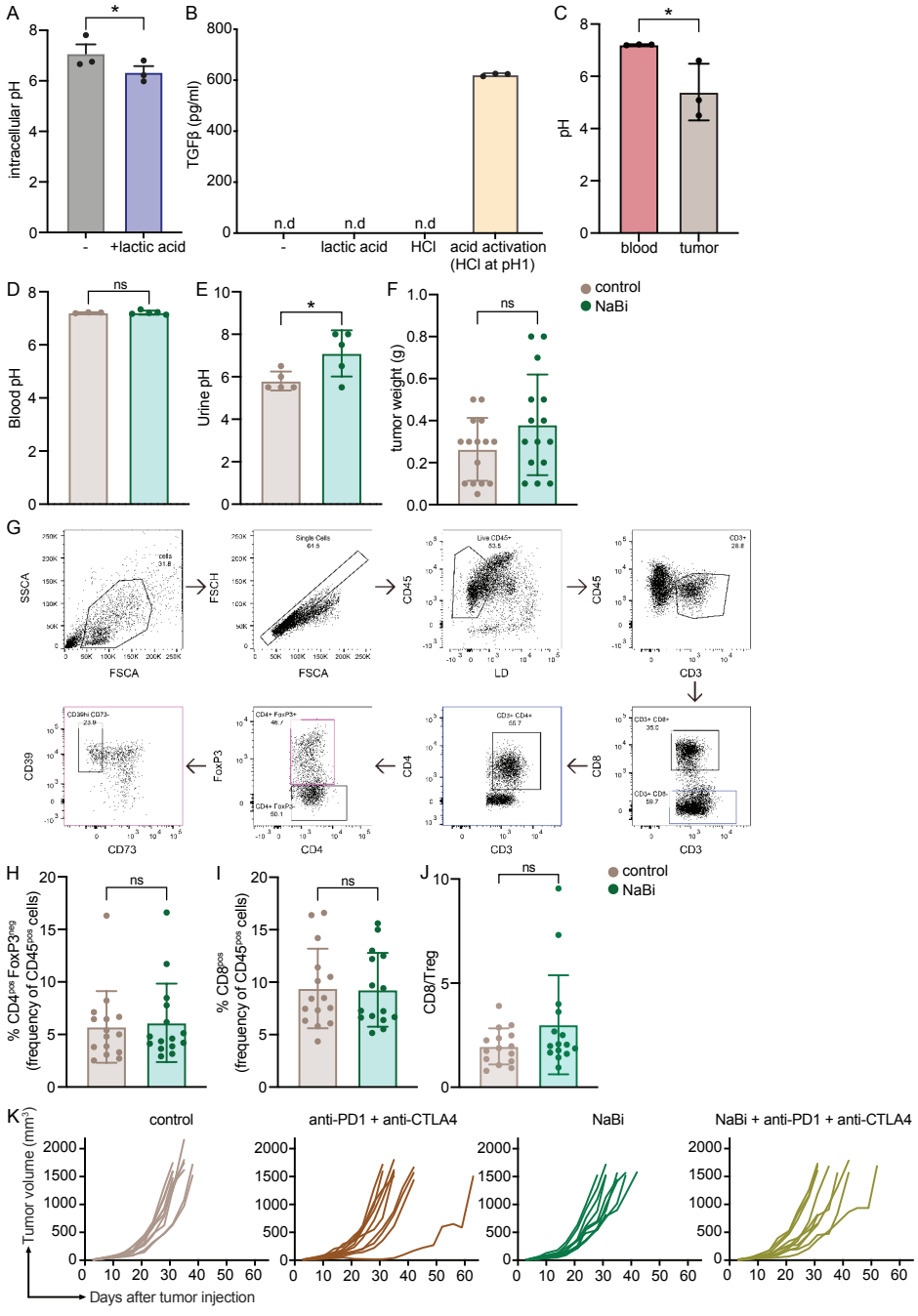

Fig S5 (supplement to figure 4): The effect of lactic acid on conversion to FoxP3⁺ cells is pH dependent
(A) Intracellular pH calculated using intensity of BCECF staining of bulk iTregs on day 3, induced in the presence of TGFβ using kit purified CD4⁺ CD25⁻ Tconv cells in low glucose condition ± lactic acid (n=3 independent experiments with at least two technical replicates within each experiment). Each dot is one independent experiment and error bars represent SEM. (B) Level of active form of TGFβ measured by ELISA

in complete culture media treated with lactic acid/hydrochloric acid (HCl) (n=3 technical replicates). n.d not detected/below the detection limit of ELISA. (C-E) pH, at the time of harvest (day 22 after tumor injection), in MeVa2.1.dOVAtumor bearing mice, treated with sodium bicarbonate (NaBi) or control drinking water. (C) pH in blood and tumor of control mice (n=3 mice); (D) pH in blood (n=3 in control and n=5 mice in NaBi group) and (E) urine (n=5 mice per group). (F) Weight of MeVa2.1.dOVA tumors across groups at endpoint (day 19 after tumor injection; n=15 mice per group). (G) Gating strategy for tumor samples: Cells were first gated based on scatter followed by doublet exclusion. This was followed by excluding dead cells and gating for CD45 positive cells. CD3 cells within this population were then gated followed by evaluating T cell subsets based on expression of CD8, CD4 and FoxP3 as indicated. Cells expressing $CD39^{hi}$ and negative for CD73 were gated within the $CD4^{+}FoxP3^{+}$ population. (H-J) Flow cytometry analysis of MeVa2.1.dOVA tumors from NaBi/vehicle treated mice at endpoint (day 19 after tumor injection) indicating (H) percentage of $CD4^{+}$ $FoxP3^{-}$ (Tconv) cells (I) $CD8^{+}$ T cells and (J) ratio of CD8 and Treg (n=15 mice per group). Each dot represents one mouse. (K) MeVa2.1.dOVA tumor volume of individual mice until endpoint (tumor volume ≥ 1500 mm^3), treated with combinations of NaBi and anti-PD-1+anti-CTLA-4 or the respective isotype control antibodies. Error bars indicate SD, unless otherwise stated. pos (+); neg (-); Statistical significance was determined using two-tailed paired Student's t-test (for A) or by two-tailed unpaired Student's t-test (for C-F) or by two-tailed unpaired Mann-Whitney U test (for H-J). ns not significant, * *p*-value<0.05.